



Regional heterogeneities in the emission of airborne primary sugar compounds and biogenic secondary organic aerosols in the East Asian outflow: evidence for coal combustion as a source of levoglucosan

Md. Mozammel Haque^{1,2,3}, Yanlin Zhang^{1,2}, Srinivas Bikkina⁴, Meehye Lee⁵, and Kimitaka Kawamura^{3,4}

¹Yale-NUIST Center on Atmospheric Environment, International Joint Laboratory on Climate and Environment Change (ILCEC), Nanjing University of Information Science & Technology, Nanjing 210044, China

²School of Applied Meteorology, Nanjing University of Information Science & Technology, Nanjing 210044, China

³Institute of Low Temperature Science, Hokkaido University, Sapporo 060-0819, Japan

⁴Chubu Institute for Advanced Studies, Chubu University, Kasugai 487-8501, Japan

⁵Department of Earth and Environmental Sciences, Korea University, Anam-dong, Sungbuk-gu, Seoul 136-701, South Korea

Correspondence: Yanlin Zhang (dryanlinzhang@outlook.com) and Kimitaka Kawamura (kkawamura@isc.chubu.ac.jp)

Received: 25 May 2021 – Discussion started: 15 June 2021

Revised: 1 December 2021 – Accepted: 7 December 2021 – Published: 27 January 2022

Abstract. Biomass burning (BB) significantly influences the chemical composition of organic aerosols (OAs) in the East Asian outflow. The source apportionment of BB-derived OA is an influential factor for understanding their regional emissions, which is crucial for reducing uncertainties in their projected climate and health effects. We analyzed here three different classes of atmospheric sugar compounds (anhydrosugars, primary sugars, and sugar alcohols) and two types of biogenic secondary organic aerosol (BSOA) tracers (isoprene- and monoterpene-derived SOA products) from a year-long study that collected total suspended particulate matter (TSP) from an island-based receptor site in Gosan, South Korea. We investigate the seasonal variations in the source emissions of BB-derived OA using mass concentrations of anhydrosugars and radiocarbon (^{14}C -) isotopic composition of organic carbon (OC) and elemental carbon (EC) in ambient aerosols. Levoglucosan (Lev) is the most abundant anhydrosugar, followed by galactosan (Gal), and mannosan (Man). Strong correlations of Lev with Gal and Man, along with their ratios (Lev/Gal is 6.65 ± 2.26 ; Lev/Man is 15.1 ± 6.76) indicate the contribution from hardwood burning emissions. The seasonal trends revealed that the BB impact is more pronounced in winter and fall, as evidenced by the high concentrations of anhydrosugars. Likewise, significant correlations among three primary sugars (i.e., glucose, fructose, and sucrose) emphasized the contribution of airborne pollen. The primary sugars showed higher concentrations in spring/summer than winter/fall. The fungal spore tracer compounds (i.e., arabinol, mannitol, and erythritol) correlated well with trehalose (i.e., a proxy for soil organic carbon), suggesting the origin from airborne fungal spores and soil microbes in the East Asian outflow. These sugar alcohols peaked in summer, followed by spring/fall and winter. Monoterpene-derived SOA tracers were most abundant compared to isoprene SOA tracers. Both BSOA tracers were dominant in summer, followed by fall, spring, and winter. The source apportionment based on multiple linear regressions and diagnostic mass ratios together revealed that BB emissions mostly contributed from hardwood and crop residue burning. We also found significant positive linear relationships of ^{14}C -based nonfossil- and fossil-derived organic carbon fractions

with Lev C, along with the comparable regression slopes, suggesting the importance of BB and coal combustion sources in the East Asian outflow.

1 Introduction

Organic aerosols (OAs), which account for a major fraction of up to 50 % of airborne total suspended particulate matter, have considerable effects on regional and global climate by absorbing or scattering sunlight (Kanakidou et al., 2005). However, the climate effects of OAs are involved with large uncertainties due to our limited understanding of the contributing sources. OAs can be derived from both primary emissions and secondarily formed species. Sugars are an important group of water soluble, primary organic compounds whose concentrations are significant in atmospheric aerosols over the continent (Jia and Fraser, 2011; Fu et al., 2008; Yttri et al., 2007; Graham et al., 2003). Anhydrosugars, such as levoglucosan, galactosan, and mannosan, are the key tracers of biomass burning (BB) emissions (Simoneit, 2002). Sugar alcohols, along with glucose, trehalose, and sucrose mostly originate from primary biological particles such as fungal spores, pollen, bacteria, viruses, and vegetative debris (Graham et al., 2003; Simoneit et al., 2004a; Bauer et al., 2008; Deguillaume et al., 2008). Primary sugars and sugar alcohols are predominantly present in the coarse-mode aerosols, accounting for 0.5 %–10 % of atmospheric aerosol carbon matter (Yttri et al., 2007; Pio et al., 2008).

Secondary organic aerosol (SOA) is a large fraction of OAs, while there were only limited studies about the key factors controlling SOA formation. The SOA formation significantly increases with the enhancement of the ambient aerosol mass (Liu et al., 2018). SOA is formed by both homogenous and heterogeneous reactions of volatile organic compounds (VOCs) in the atmosphere (Surratt et al., 2010; Robinson et al., 2007; Claeys et al., 2004). On a global estimation, biogenic VOCs (BVOCs) such as isoprene, monoterpenes (e.g., α/β -pinene), and sesquiterpenes (e.g., β -caryophyllene) are 1 order of magnitude higher than those of anthropogenic VOCs (e.g., toluene; Guenther et al., 2006). The global emissions of annual BVOCs were estimated to be $1150 \text{ Tg C yr}^{-1}$, accounting for 44 % isoprene and 11 % monoterpenes (Guenther et al., 1995). Isoprene is highly reactive and promptly reacts with oxidants such as O_3 , OH, and NO_x in the atmosphere to form SOA (Kroll et al., 2005, 2006; Ng et al., 2008; Surratt et al., 2010; Bikkina et al., 2021), estimated to be $19.2 \text{ Tg C yr}^{-1}$, consisting of ~ 70 % of the total SOA budget (Heald et al., 2008). Monoterpenes are important sources of biogenic secondary organic aerosol (BSOA), considering α -pinene as major species, accounting for ~ 35 % of the global monoterpenes emissions (Griffin et al., 1999).

Anthropogenic activities such as coal and biofuel combustion over East Asia, including China, are responsible for

the vast emission of OA (Huebert et al., 2003; Zhang et al., 2016). Understanding the ambient levels of OA in the East Asian outflow is crucial for assessing their regional climatic effects. As part of this effort, the Korean Climate Observatory at Gosan (KCOG), a supersite located in South Korea, is an ideal location for investigating the atmospheric outflow characteristics from East Asia (P. Fu et al., 2010; Kundu et al., 2010; Ramanathan et al., 2007; Kawamura et al., 2004; Arimoto et al., 1996). For instance, primary OA associated with soil/desert dust in East Asia, along with forest fires in Siberia/northeastern China, are transported over Gosan in the spring (G. H. Wang et al., 2009). BSOA during long-range transport from the continent and open ocean, as well as local vegetation, can significantly contribute to Gosan aerosols. Although these investigations were carried out almost a decade ago, no such observations are available in contemporary times from Gosan. Here, we attempt to understand the current states of East Asian OAs using both the molecular marker approach and radiocarbon data of carbonaceous components.

The KCOG, located on the western side of Jeju Island adjacent to the Yellow Sea and the East China Sea, is facing the Asian continent but is isolated from public areas of the island (Kawamura et al., 2004). Simoneit et al. (2004b) documented, during the Aerosol Characterization Experiment (ACE-Asia) field campaign, that OAs from BB and fossil fuel combustion sources are transported along with desert dust to the KCOG during continental outflow. An intensive campaign was organized at the KCOG during spring 2005 to observe the physical properties of East Asian aerosols while two dust events were detected (Nakajima et al., 2007). Here, we focus on the characterization of airborne anhydrosugars, primary sugars, sugar alcohols, and BSOA tracers from the KCOG. Gosan is influenced by the continental outflow from East Asia during winter, spring, and fall, whereas the site is influenced by the maritime air masses from the Pacific Ocean and other marginal seas during summer. This makes the KCOG ideal for characterizing the regional heterogeneities in the emissions of organic compounds in the East Asian outflow based on the total suspended particulate (TSP) samples collected during April 2013–April 2014.

2 Methods

2.1 Aerosol sampling and prevailing meteorology

TSP samples were collected on precombusted (450°C for 6 h) quartz fiber filters ($20 \text{ cm} \times 25 \text{ cm}$; Pallflex) at the KCOG (33.17° N , 126.10° E ; see Fig. 1), South Korea. To ob-

tain enough signal for the radiocarbon measurements, each TSP sample was collected for 10–14 d from April 2013 to April 2014. A total of 21 samples were collected using a high-volume air sampler (Kimoto AS-810; $\sim 65 \text{ m}^3 \text{ h}^{-1}$) installed on the rooftop of a trailer house ($\sim 3 \text{ m}$ above the ground). After the collection, the aerosol filters were transferred to a precombusted (450°C for 6 h) glass jar (150 mL) equipped with a Teflon-lined screw cap and transported to the laboratory in Sapporo. These TSP samples were stored in a dark freezer room at -20°C until the analysis. Three field blank filters were also collected during the campaign.

The ambient temperatures at the Gosan site were, on average, 6.9°C in winter, 14.1°C in spring, 27.0°C in summer, and 17.1°C in fall. Likewise, the average relative humidity was found to be highest in summer (71.3 %), followed by spring (64.9 %), fall (63.5 %), and winter (54.7 %). Gosan is influenced by the pollution sources in East Asia during winter and other transition periods (spring and fall) due to the prevailing westerlies. In contrast, winds in summer blew mostly from the western North Pacific (WNP) by the easterly winds. The spring season is, in particular, important for the transport of mineral dust mixed with polluted OAs to Gosan (Kundu et al., 2010).

2.2 Extraction and analysis of organic compounds

Approximately 3.14 cm^2 filter cuts were extracted with dichloromethane/methanol (2 : 1; v/v). The extracts were concentrated using a rotary evaporator under vacuum and then blown down to near-dryness with pure nitrogen gas. The dried residues were subsequently reacted with N, O-bis(trimethylsilyl)trifluoroacetamide containing 1 % trimethylchlorosilane (BSTFA + 1 % TMCS; Supelco®, Sigma-Aldrich) and pyridine at 70°C for 3 h to derive OH and COOH groups of polar organic compounds to trimethylsilyl ethers and esters, respectively. After the derivatization followed by the addition of a known amount of internal standard solution (Tridecane; 1.43 ng L^{-1} in *n*-hexane), the derivatized extracts were injected onto a gas chromatograph (GC; Hewlett Packard model 6890) coupled to a mass spectrometer (GC-MS; Hewlett Packard model 5973). More details on the quantification of polar organic compounds using GC-MS are described in Haque et al. (2019).

The target compounds (anhydrosugars, primary sugars, sugar alcohols, and BSOA tracers) were separated on a DB-5ms fused silica capillary column ($30 \text{ m} \times 0.25 \text{ mm}$ internal diameter; $0.5 \mu\text{m}$ film thickness) using helium as a carrier gas at a flow rate of 1.0 mL min^{-1} . The GC oven temperature was programmed from 50°C for 2 min and then increased from 50 to 120°C at $30^\circ\text{C min}^{-1}$ and to 300°C at 6°C min^{-1} , with a final isotherm hold at 300°C for 16 min. The sample was injected in a splitless mode with the injector temperature at 280°C . The MS was operated at 70 eV and scanned from 50 to 650 Da on an electron impact (EI) mode. Mass spectral data (MSD) were acquired and processed using

ChemStation software. The organic compounds were identified individually by comparison with retention times and mass spectra of authentic standards and NIST Library and the literature data of mass fragmentation patterns (Medeiros and Simoneit, 2007). For assessing the recoveries, ~ 100 – 200 ng of the standard solution was spiked on the blank filter and analyzed as a real sample. Overall, the average recoveries were found to be 80 %–104 % for target compounds. The field and laboratory blank filters ($n = 3$) were also analyzed by the same procedures as a real sample. Target compounds were not found in the field blanks. The analytical errors based on concentrations by replicate sample analyses ($n = 3$) were less than 15 %.

2.3 Carbon fractions analysis

Organic carbon (OC) and elemental carbon (EC) were analyzed using a thermal–optical transmittance method with a Sunset Laboratory carbon analyzer, following the NIOSH (National Institute for Occupational Safety and Health) protocol (Birch and Cary, 1996), and detailed procedures were given elsewhere (Zhang et al., 2016). Furthermore, a portion of 2.54 cm^2 of each sample filter was extracted with 15 mL ultrapure water (resistivity $> 18.2 \text{ M}\Omega \text{ cm}$; Sartorius Arium 611 UV) with ultrasonication for 30 min. The water extracts were then filtered through a membrane disk filter for water soluble organic carbon (WSOC) analysis by a total organic carbon (TOC) analyzer (Shimadzu TOC-VCSH; Boreddy et al., 2018). The concentrations of WSOC were corrected by field blanks. The analytical errors in the triplicate analyses were less than 5 % for WSOC.

2.4 Radiocarbon isotopic composition of total carbon and EC

The concentrations of total carbon (TC) in the TSP samples were determined using an elemental analyzer. For the radiocarbon isotopic composition ($\Delta^{14}\text{C}$), the aerosol filter punches (1.5 cm^2) were exposed for $\sim 12 \text{ h}$ to HCl fumes in a vacuum desiccator. Subsequently, the punches were analyzed for $\Delta^{14}\text{C}$ on a modified elemental analyzer coupled via a gas interface to accelerator mass spectrometer mini carbon dating system (MICADAS) at the University of Bern, Switzerland (Salazar et al., 2015). The evolved CO_2 of TC from the elemental analyzer was passed through a moisture trap (SICAPENT®, Merck KGaA) and isolated from other residual gases using a temperature-controlled zeolite trap. The purified CO_2 was introduced through a gas interface system to MICADAS, where $^{14}\text{C}/^{12}\text{C}$ ratios are measured according to the analytical procedures detailed in Zhang et al. (2016). Likewise, the evolved CO_2 of elemental carbon from the Sunset Laboratory OC/EC analyzer, using the Swiss 4S protocol (Zhang et al., 2012), was directed to the MICADAS and measured for the $^{14}\text{C}/^{12}\text{C}$ ratio relative to standard calibration gas. These results were expressed as fractions of modern

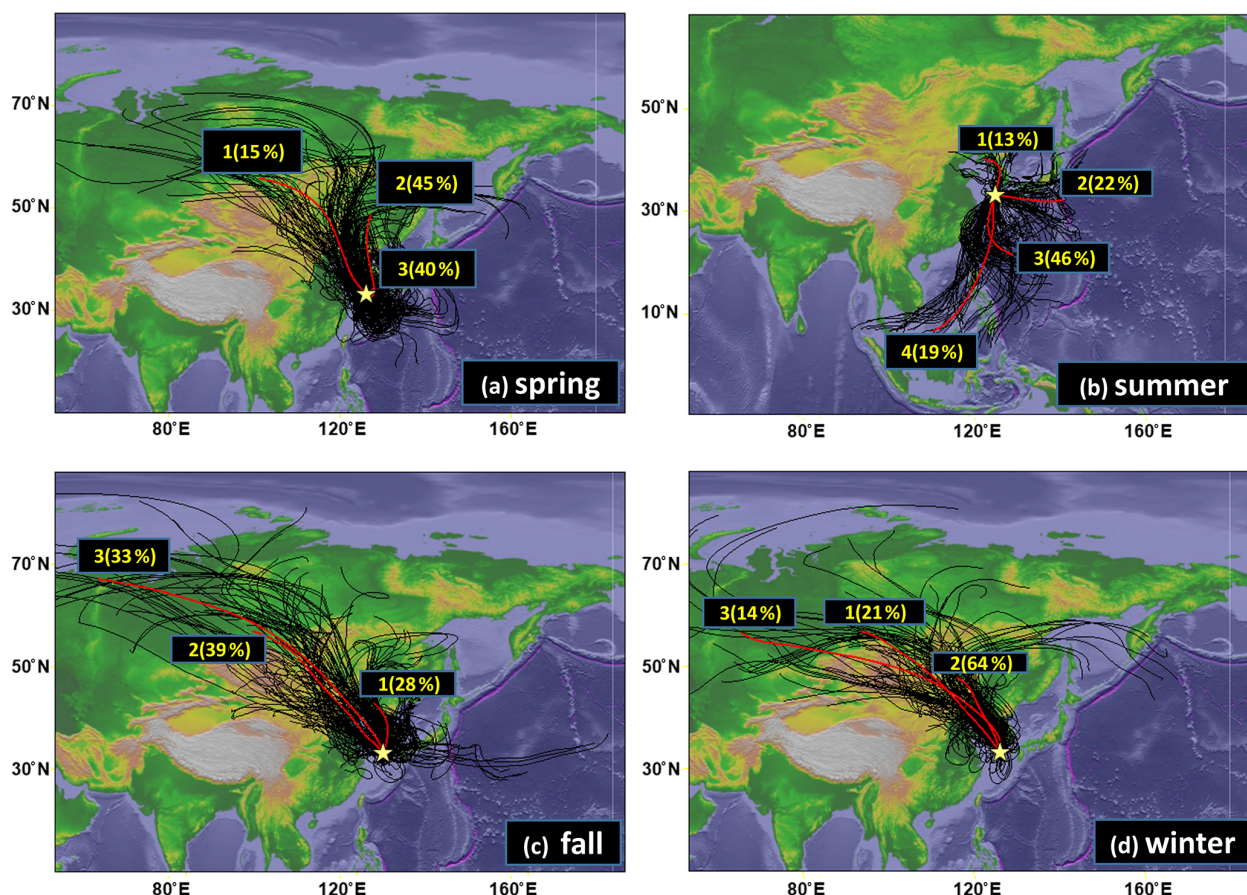


Figure 1. Cluster analysis of backward air mass trajectories over Gosan (indicated by a star) for the TSP collected during the (a) spring, (b) summer, (c) fall, and (d) winter seasons.

carbon (f_M) by normalizing with a $\delta^{13}\text{C}$ value of the reference standard in the year 1950 (-25‰), according to Stuiver and Polach (1997), for the fractionation effects. The $f_M(\text{OC})$ can be estimated by using the $f_M(\text{TC})$ and $f_M(\text{EC})$ in an isotope mass balance equation (Zhang et al., 2015). Additionally, we estimated the relative contributions of OC and EC from the nonfossil and fossil sources ($f_{\text{nonfossil}}$ and f_{fossil} , respectively) using the following equations.

$$f_{\text{nonfossil-OC}} = f_M(\text{OC-sample})/f_M(\text{OC-ref}); f_M(\text{OC-ref}) \approx 1.07 \pm 0.04 \quad (1)$$

$$f_{\text{nonfossil-EC}} = f_M(\text{EC-sample})/f_M(\text{EC-ref}); f_M(\text{EC-ref}) \approx 1.10 \pm 0.05 \quad (2)$$

$$f_{\text{fossil-OC}} = 1 - f_{\text{nonfossil-OC}} \quad (3)$$

$$f_{\text{fossil-EC}} = 1 - f_{\text{nonfossil-EC}} \quad (4)$$

The reference values of OC and EC were obtained from Mohn et al. (2008). Using the fractions of $f_{\text{fossil-OC}}$ and $f_{\text{nonfossil-OC}}$, we can, therefore, estimate the mass concentration of ambient organic carbon ($\text{OC}_{\text{ambient}}$) from fossil and

nonfossil sources ($\text{OC}_{\text{fossil}}$ and $\text{OC}_{\text{nonfossil}}$, respectively).

$$\text{OC}_{\text{nonfossil}} = f_{\text{nonfossil-OC}} \times [\text{OC}]_{\text{ambient}} \quad (5)$$

$$\text{OC}_{\text{fossil}} = f_{\text{fossil-OC}} \times [\text{OC}]_{\text{ambient}} \quad (6)$$

More details on the radiocarbon isotopic composition data over Gosan were reported elsewhere (Zhang et al., 2016).

3 Results and discussion

3.1 Trajectory and cluster analysis

Backward air mass trajectories are useful for assessing the impact of local versus regional source emissions over Gosan. The 7 d isentropic backward air mass trajectories were computed using the Hybrid Single-Particle Lagrangian Integrated Trajectory model (HYSPLIT, version 4; Stein et al., 2015) over the KCOG for the sampling period using the meteorological datasets of the Global Data Assimilation System (GDAS) network. The trajectory endpoint files from the HYSPLIT model were further used for the cluster analysis using the TrajStat package (Y. Q. Wang et al., 2009) for all four seasons (Fig. 1). Although cluster analysis revealed the

predominance of continental transport in the spring, fall, and winter seasons, the air masses over the KCOG in summer mostly originated from the WNP. Since spring is a transition of winds switching from westerlies to easterlies, Gosan is likely influenced by the long-range transport of dust, pollution, and sea salt aerosols.

The vertical mixing of pollutants within the boundary layer height also plays an important role in controlling the strength of continental outflow alongside regional meteorology. For instance, the mixing height of air parcels from the HYSPLIT model is mostly confined to 1000 m in winter but somewhat increased towards the spring and fall seasons (Fig. S1 in the Supplement). This vertical enhancement in the boundary layer height facilitates the transport of mineral dust particles from the arid and semiarid regions in East Asia along with urban pollutants to Gosan in spring and fall compared to winter. However, the strength of the continental outflow somewhat depends on several factors, including the source emissions, meteorology, and mixing height of air parcels.

Gosan is influenced by three types of air masses in spring (Fig. 1a), from the Gobi Desert (cluster 1 is 15 %), North China (cluster 2 is 45 %), and from the Yellow Sea (cluster 3 is 40 %). In contrast, the easterlies from the WNP in summer mostly influenced the composition of TSP over the KCOG. This inference is based on the cluster analysis for summer samples (Fig. 1b), which showed four regimes, including transport from the Sea of Japan (cluster 1 is 13 %), WNP (cluster 2 is 22 %), South China Sea (cluster 3 is 46 %), and East China Sea (cluster 4 is 19 %). In contrast, cluster analysis revealed three major transport regimes from East Asia in fall and winter (Fig. 1c, d). However, there are subtle differences that exist between winter and fall in terms of influence from nearby versus distant pollution sources. For instance, long-range transport of air masses from western Mongolia (cluster 1 is 21 %) and the Russian Far East (cluster 3 is 14 %) exerted a weak influence on the TSP sampled over Gosan in winter. Besides, we observed a somewhat larger impact of air masses from the North China Plain over Gosan (cluster 2 is 64 %) in winter. In contrast, Gosan is less influenced by air masses originating from the North China Plain, contributing $\sim 28\%$ (cluster 1) than those from Mongolia (cluster 2 is 39 %) and the Russian Far East (cluster 3 is 33 %) in the fall. Therefore, the impact of East Asian outflow is stronger in winter than in spring and fall.

3.2 Temporal and seasonal variability in sugars

The temporal/seasonal trends of sugar compounds over the KCOG provide useful information on the emission strengths of various sources in the East Asian outflow. All three anhydrosugars showed similar temporal and seasonal trends, with higher concentrations in winter and fall than spring and summer (Figs. 2a and S2 in the Supplement). As levoglucosan and two other anhydrosugars (mannosan and galactosan)

are the pyrolysis products of cellulose/hemicellulose, their higher concentrations, along with an increase in the nonfossil fraction of OC (Fig. 2a; pie charts) in TSP from winter and fall revealed the impact of BB emissions. The MODIS satellite-based fire counts (Fig. S1), together with cluster analysis in winter and fall (Fig. 1) have revealed an influence of active BB emissions in the North China Plain, Mongolia, and the Russian Far East. The temporal trends of glucose, fructose, and sucrose exhibited less variability throughout the sampling period; however, we observed a slight increase in their concentration towards spring/summer (Fig. 2a). Glucose and fructose have origins from leaf fragments and pollen species (P. Fu et al., 2012). Sucrose is a potential tracer for airborne pollen (P. Fu et al., 2012) and late spring/early summer is often regarded as a season of pollen allergies. Therefore, the similar temporal trends of glucose and fructose with sucrose indicate their common source, namely pollens (Fig. 2a). Since glucose, fructose, and sucrose showed moderately significant correlations ($R^2 = 0.44\text{--}0.48$; $p < 0.01$) with levoglucosan in winter, it is somewhat possible that BB source emission could also influence the concentrations of these saccharides in this season (Haque et al., 2019; Fu et al., 2008).

BB also contributes to xylose, and hence, the temporal variability in xylose is mimicking that of the anhydrosugars. Trehalose is a primary sugar and a useful tracer for organic carbon associated with soil dust particles (P. Fu et al., 2012). The temporal variability in trehalose closely resembles that of the fungal spore tracers (arabitol, mannitol, and erythritol), showing high concentrations in the spring, summer, and fall seasons (Figs. 2a and S2; Zhu et al., 2015a; P. Fu et al., 2012). The KCOG is under the influence of a large-scale advection of mineral dust from East Asia to the WNP during these three seasons (Tyagi et al., 2017; Huebert et al., 2003). The mineral dust transport from East Asia to the WNP can be traced by the high concentrations of non-sea-salt (nss) Ca^{2+} in the TSP samples from Gosan (Arimoto et al., 1996). Similar temporal trends of trehalose and nss Ca^{2+} , particularly in spring samples (Fig. S3 in the Supplement), suggest that the abundance of OAs specific to fungal spores over Gosan is likely associated with the Kosa (Asian dust) events.

The major sources of arabitol and mannitol are airborne fungal spores (Bauer et al., 2008), accompanying detritus from mature leaves (Pashynska et al., 2002). Heald and Spracklen (2009) reported that mannitol and arabitol are considerably associated with terrestrial biosphere activity. Inositol is largely derived from the developing leaves in summer (Pashynska et al., 2002) and BB in winter (P. Q. Fu et al., 2010). Zhu et al. (2015b) found a similar seasonal behavior of inositol with those of other sugar alcohols with the predominance in summer, which is associated with microbial activities in local forests from Okinawa. Inositol showed a moderately significant correlation with levoglucosan ($R^2 = 0.33$; $p < 0.01$) in winter; however, there were no positive linear relationships between levoglucosan and other sugar

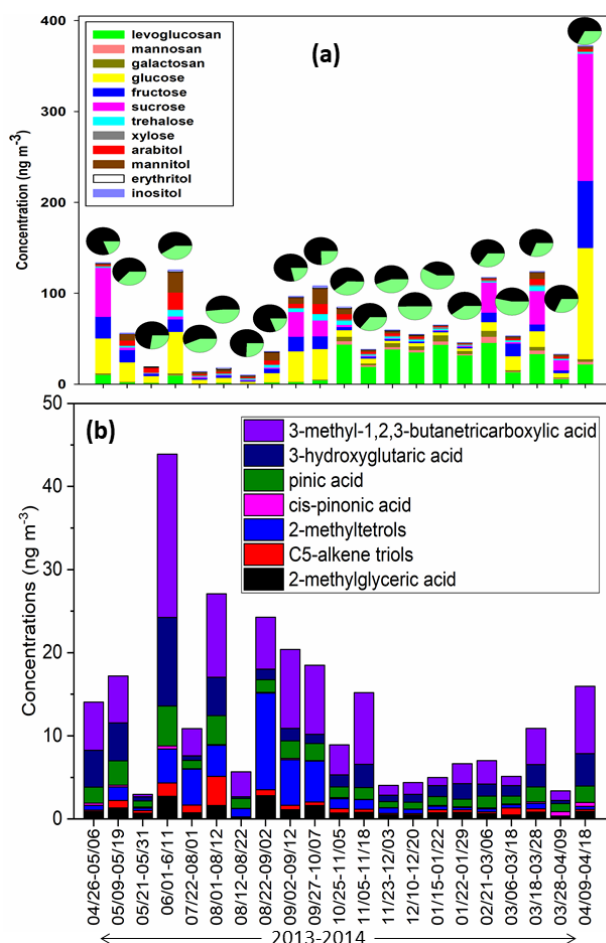


Figure 2. (a) Cumulative concentration levels of anhydrosugars, primary sugars, and sugar alcohols (i.e., represented by bars) and depicting the contributions of nonfossil (green color) and fossil (black color) organic carbon (i.e., pie charts). (b) Cumulative concentration levels of isoprene and monoterpene SOA tracers in each TSP sample collected over Gosan.

alcohols, implying a partial emission of inositol from the BB during winter in Gosan aerosols. Therefore, the temporal variability in inositol differs from that of the other sugar alcohols (Fig. S2). The sources of sugar compounds are further discussed in Sect. 3.4.

The seasonally averaged concentrations of all the anhydrosugars and xylose are higher in winter/fall than spring/summer (Fig. 3a–d), possibly due to a greater influence of long-range transport from East Asia. In contrast, glucose, fructose, and sucrose peaked in spring but decreased in the other seasons (Fig. 3e–g), mainly because of the contribution of airborne pollen. Trehalose showed higher concentrations in fall and summer, followed by spring and winter (Fig. 3h). Arabinol, mannitol, and erythritol showed higher concentrations in summer/fall than in winter and spring (Fig. 3i–k). This seasonal trend is consistent with those of soil-derived fungal spores. This feature is consistent with ear-

lier observations from a remote oceanic island in the WNP (Okinawa) during the impact of East Asian outflow (Zhu et al., 2015a). The seasonally averaged mass concentrations of inositol are highest in spring, followed by summer, fall, and winter (Fig. 3l). Overall, the molecular compositions of anhydrosugars showed the predominance of levoglucosan followed by galactosan and mannosan (Fig. S4 in the Supplement). Galactosan is more abundant in crop residue burning emissions than mannosan (Engling et al., 2009; Sheesley et al., 2003). It is very likely that the impact of crop residue burning emissions in East Asia over Gosan is more prominent in winter/spring. Such high abundances of galactosan over mannosan were found in the North China Plain (Fu et al., 2008) and in the Indo-Gangetic Plain outflow sampled over the Bay of Bengal (Bikkina et al., 2019). Although the temporal variability in primary sugars in the TSP samples from Gosan showed a characteristic peak of glucose and sucrose (Fig. 2a), the seasonally averaged distributions are different (Fig. S4). The molecular distributions of sugar alcohols are characterized by high loadings of arabinol and mannitol, followed by erythritol and inositol (Fig. S4).

3.3 Temporal and seasonal variability in BSOA tracers

We identified six isoprene SOA tracers such as 2-methylglyceric acid (2-MGA), three C₅-alkene triols, and two 2-methyltetrols (2-methylthreitol and 2-methylethritol – 2-MTs) in Gosan aerosol samples (Table 1). The sum of the isoprene SOA tracers ranged from 0.35 to 15.1 ng m⁻³ (avg. 3.69 ng m⁻³), with the predominance of 2-MTs (avg. 2.09 ng m⁻³). 2-MGA is the second most abundant isoprene SOA tracer (avg. 0.99 ng m⁻³) and is a high-generation product probably formed by further photooxidation of methacrolein and methacrylic acid. A similar molecular composition was observed over the North Pacific and California coast (Fu et al., 2011). All the isoprene SOA tracers exhibited similar temporal variations, with higher concentrations in the summer/spring months compared to fall and winter (Fig. 2b). Conversely, four monoterpene SOA tracers, i.e., *cis*-pinonic acid, pinic acid, 3-hydroxyglutaric acid (3-HGA), and 3-methyl-1,2,3-butanetricarboxylic acid (MBTCA), were detected in the Gosan samples (Table 1). The total concentrations of monoterpene SOA tracers were found to be 1.65 to 35.5 ng m⁻³ (avg. 9.24 ng m⁻³), with a high concentration of MBTCA (avg. 5.11 ng m⁻³). All the monoterpene SOA tracers showed similar temporal trends, with high values in summer/spring periods than fall/winter (Fig. 2b). Nevertheless, *cis*-pinonic acid exhibited a somewhat different temporal variability than the other monoterpene SOA tracers. It is likely that *cis*-pinonic acid might be further photooxidized to form MBTCA (Szmigielski et al., 2007).

The seasonal average of isoprene SOA tracers showed high concentrations in summer, followed by spring/fall and winter (Fig. 3m–o). One key feature of the data presented

Table 1. Concentrations of identified sugar compounds and BSOA tracers (nanograms per cubic meter; hereafter ng m^{-3}) in the atmospheric aerosol samples from Gosan.

| Species | Annual (avg. ^a \pm SD ^b , min. ^c , max. ^d) | Summer (avg. \pm SD, min., max.) | Fall (avg. \pm SD, min., max.) | Winter (avg. \pm SD, min., max.) | Spring (avg. \pm SD, min., max.) |
|---------------------------|---|--|--|--|--|
| Anhydrosugars | | | | | |
| Levogluconan (Lev) | 17.6 \pm 16.8 0.60, 45.9 | 2.92 \pm 3.89 0.60, 9.81 | 21.7 \pm 19.0 2.30, 43.9 | 39.2 \pm 6.60 32.0, 45.9 | 12.7 \pm 11.6 1.45, 33.4 |
| Mannosan (Man) | 1.57 \pm 1.82 0.05, 6.74 | 0.18 \pm 0.24 0.05, 0.61 | 1.69 \pm 1.49 0.13, 3.66 | 3.63 \pm 2.28 1.47, 6.74 | 1.31 \pm 1.57 0.08, 4.08 |
| Galactosan (Gal) | 2.28 \pm 2.10 0.14, 6.78 | 0.64 \pm 0.68 0.14, 1.82 | 2.45 \pm 2.13 0.35, 4.92 | 5.21 \pm 1.64 3.40, 6.78 | 1.65 \pm 1.26 0.50, 3.88 |
| Primary sugars | | | | | |
| Glucose | 18.8 \pm 27.1 2.45, 122 | 13.4 \pm 18.2 2.45, 45.6 | 16.5 \pm 15.7 2.68, 33.6 | 4.74 \pm 3.14 2.88, 9.44 | 32.4 \pm 41.1 4.87, 122 |
| Fructose | 10.3 \pm 15.9 0.97, 74.0 | 4.90 \pm 5.15 0.97, 13.7 | 7.48 \pm 6.99 1.71, 16.2 | 3.82 \pm 4.45 1.56, 10.5 | 19.8 \pm 25.0 2.69, 74.0 |
| Sucrose | 16.1 \pm 32.2 0.26, 140 | 1.46 \pm 1.05 0.68, 3.28 | 9.74 \pm 12.1 0.76, 27.2 | 8.87 \pm 16.3 0.42, 33.3 | 35.1 \pm 50.5 0.26, 140 |
| Trehalose | 2.42 \pm 1.97 0.65, 7.03 | 2.72 \pm 2.53 0.97, 6.98 | 3.71 \pm 2.29 1.18, 7.03 | 1.21 \pm 0.42 0.72, 1.63 | 1.98 \pm 1.55 0.65, 5.33 |
| Xylose | 0.81 \pm 0.65 0.04, 2.03 | 0.23 \pm 0.23 0.04, 0.63 | 0.86 \pm 0.68 0.14, 1.70 | 1.59 \pm 0.37 1.21, 2.03 | 0.74 \pm 0.55 0.16, 1.68 |
| Sugar alcohols | | | | | |
| Arabitol | 3.96 \pm 4.24 0.47, 18.7 | 5.64 \pm 7.46 1.20, 18.7 | 5.27 \pm 3.51 2.27, 10.9 | 1.06 \pm 0.60 0.47, 1.91 | 3.47 \pm 2.19 1.18, 6.30 |
| Mannitol | 4.61 \pm 5.54 0.25, 22.0 | 7.39 \pm 8.65 1.71, 22.0 | 6.64 \pm 6.03 1.69, 16.7 | 0.99 \pm 0.45 0.55, 1.60 | 3.24 \pm 2.67 0.25, 7.03 |
| Erythritol | 0.62 \pm 0.43 0.12, 1.52 | 0.92 \pm 0.53 0.42, 1.52 | 0.93 \pm 0.33 0.55, 1.27 | 0.42 \pm 0.27 0.16, 0.80 | 0.30 \pm 0.12 0.12, 0.48 |
| Inositol | 0.34 \pm 0.39 0.04, 1.53 | 0.29 \pm 0.41 0.08, 1.03 | 0.56 \pm 0.60 0.10, 1.53 | 0.13 \pm 0.07 0.08, 0.23 | 0.35 \pm 0.28 0.04, 0.73 |
| Isoprene SOA tracers | | | | | |
| 2-MGA | 0.99 \pm 0.70 0.17, 2.79 | 1.61 \pm 1.17 0.17, 2.79 | 0.95 \pm 0.43 0.51, 1.61 | 0.67 \pm 0.14 0.49, 0.81 | 0.76 \pm 0.35 0.20, 1.32 |
| Σ 2-MLTs | 1.04 \pm 1.40 0.05, 5.81 | 2.48 \pm 1.98 0.51, 5.81 | 1.34 \pm 1.16 0.33, 2.74 | 0.20 \pm 0.05 0.15, 0.26 | 0.29 \pm 0.25 0.05, 0.82 |
| Σ C5-alkene triols | 0.20 \pm 0.25 0.02, 1.17 | 0.46 \pm 0.44 0.02, 1.17 | 0.13 \pm 0.05 0.05, 0.18 | 0.09 \pm 0.03 0.05, 0.13 | 0.14 \pm 0.11 0.02, 0.30 |
| Monoterpene SOA tracers | | | | | |
| <i>Cis</i> -pinonic acid | 0.15 \pm 0.14 0.02, 0.52 | 0.12 \pm 0.13 0.03, 0.36 | 0.08 \pm 0.06 0.02, 0.16 | 0.07 \pm 0.03 0.02, 0.10 | 0.26 \pm 0.17 0.08, 0.52 |
| Pinic acid | 1.67 \pm 1.01 0.72, 4.81 | 2.40 \pm 1.67 0.99, 4.81 | 1.53 \pm 0.57 0.75, 2.11 | 1.07 \pm 0.25 0.84, 1.42 | 1.61 \pm 0.78 0.72, 2.94 |
| 3-HGA | 2.30 \pm 2.38 0.19, 10.6 | 3.46 \pm 4.39 0.19, 10.6 | 1.52 \pm 0.77 0.76, 2.79 | 1.40 \pm 0.39 0.94, 1.88 | 2.54 \pm 1.83 0.38, 4.57 |
| MBTCA | 5.11 \pm 4.54 0.29, 19.6 | 8.44 \pm 6.88 3.00, 19.6 | 6.24 \pm 3.64 1.17, 9.49 | 1.90 \pm 0.85 0.97, 2.83 | 3.77 \pm 2.96 0.29, 8.08 |

^a Average, ^b standard deviation, ^c minimum, ^d maximum. 2-MGA – 2-methylglyceric acid; 2-MLTs – 2-methyltetrols; 3-HGA – 3-hydroxyglutaric acid; MBTCA – 3-methyl-1,2,3-butanetricarboxylic acid.

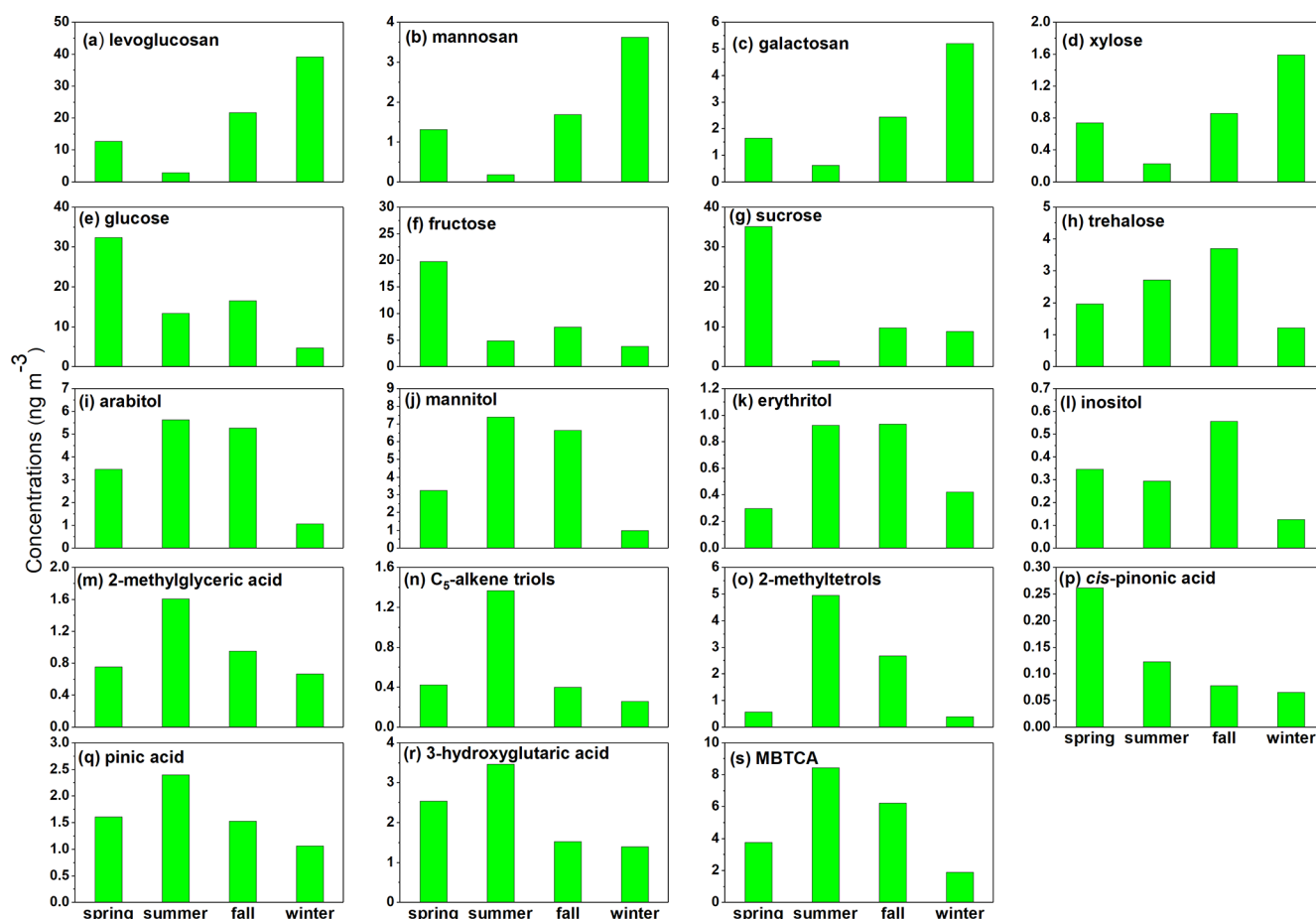


Figure 3. Seasonal variability in the atmospheric levels of sugar compounds and BSOA tracers in TSP samples from Gosan during April 2013–April 2014.

here is that two fall samples (KOS984 for 2–12 September and KOS986 for 27 September to 7 October) exhibited high concentrations for 2-MTs over Gosan (Fig. 2b). We presumed that local vegetation might contribute significantly to the formation of 2-MTs, as they are first-generation products. Moreover, 2-MTs can be derived from the open ocean under low NO_x conditions (Hu et al., 2013). 3-HGA and pinic acid showed somewhat higher concentrations in summer/spring than fall/winter due to the growing vegetation (Fig. 3q, r). *Cis*-pinonic acid was more abundant in spring compared to summer (Fig. 3p) because of its photodegradation, as discussed above. In contrast, MBTCA was more dominant in summer/fall than in spring/winter (Fig. 3s). Here, the formation of MBTCA could be enhanced in fall during atmospheric transport from East Asia. The molecular distributions of isoprene SOA tracers were characterized by a high loading of 2-MTs, followed by 2-MGA and C_5 -alkene triols in all seasons (Fig. S4). The molecular composition of monoterpene SOA tracers was dominated by MBTCA, followed by 3-HGA, pinic acid, and *cis*-pinonic acid in all seasons (Fig. S4). Overall, BSOA tracers were found to be most

abundant in summer, followed by fall, spring, and winter (Table 1). Interestingly, it is likely that secondary OA undergoes much faster cycling than the primary sugar compounds, considering the feasibility of photooxidation. This would mean a slight underestimation of BSOA over the KCOG in the East Asian outflow, and hence, their atmospheric abundances over Gosan reflect a lower limit.

Kang et al. (2018b) reported that monoterpene SOA tracers were more abundant than isoprene SOA tracers in spring–summer over the East China Sea, which is consistent with this study. Although the mass budget calculations showed that isoprene and monoterpenes are largely emitted by terrestrial plants, the open ocean can also contribute to isoprene and monoterpenes significantly (Conte et al., 2020; Shaw et al., 2010; Broadgate et al., 1997). Air mass back trajectory and cluster analysis (Fig. 1) implied that the air masses mostly originated from the ocean during summer. This means the open ocean significantly contributed to isoprene SOA production. However, terrestrial sources from the continent also substantially enhanced the formation of BSOA. For example, one sample (KOS979; 1–11 June 2013) during sum-



Figure 4. Multiple linear regression (MLR) analysis of airborne sugar compounds in TSP collected over Gosan.

mer showed the highest loading of BSOA tracers (Fig. 2b) when air masses were transported from the continent (Zhang et al., 2016).

3.4 Source apportionment – regression analysis and diagnostic ratios

The anhydrosugars strongly correlated with xylose (Fig. 4), suggesting their common source as BB emission in East Asia. P. Fu et al. (2012) analyzed pollen from different tree species (e.g., Japanese white birch (*Betula platyphylla*), Chi-

nese willow (*Salix matsudana*), weeping willow (*Salix babylonica*), sugi (*Cryptomeria japonica*), and hinoki cypress (*Chamaecyparis obtusa*), which are enriched with sucrose ($182\text{--}37\,300\,\mu\text{g g}^{-1}$), glucose ($378\text{--}3601\,\mu\text{g g}^{-1}$), and fructose ($162\text{--}1813\,\mu\text{g g}^{-1}$). In our samples, sucrose strongly correlated with glucose and fructose (Fig. 4), suggesting their origin from plant-derived airborne pollen. Likewise, a strong correlation was found between arabinol and mannitol, indicating a mutual origin from a similar type of fungal spores (Zhu et al., 2015a; P. Fu et al., 2012; Bauer et al., 2008;

Yttri et al., 2007). Bauer et al. (2008) ascribed weak correlations between arabitol and mannitol to the diverse nature of ambient fungal spores. Furthermore, both sugar alcohols correlated well with trehalose, a tracer for soil organic carbon (P. Fu et al., 2012). This observation suggests their common origin from soil organic matter associated with fungal spores. Erythritol also originates from fungal spores; however, its abundance is affected by the atmospheric aging process. Kessler et al. (2010) reported that erythritol is degraded during long-range transport in 12.7 d. Consequently, arabitol and mannitol were moderately correlated with erythritol in the Gosan samples due to the degradation of the latter sugar alcohol in the East Asian outflow.

The linear relationship of levoglucosan (Lev) with mannosan (Man), galactosan (Gal), and nss K^+ provides useful information on the type of BB emissions (hardwood, softwood, or crop residue). Ratios of Lev/Man and Lev/(Man + Gal) can be useful to distinguish BB and coal combustion contributions. The average ratios of Lev/Man (15.1 ± 6.76) and Lev/(Man + Gal) (4.27 ± 1.23) in Gosan aerosols are much closer to those from wood burning and coal combustion sources emissions, respectively (Yan et al., 2018). It reveals that Lev could originate from both biomass and coal burning source emissions, which is consistent with the linear relationship between Lev C and the fossil/nonfossil carbon fraction (Sect. 3.6). Furthermore, different types of biomass are characterized by distinct Lev/Man ratios. For instance, Lev/Man ratios from the softwood burning emissions (3–10) differ from those of hardwood (15–25) and crop residues (> 40 ; Singh et al., 2017; Schmidl et al., 2008a, b; Fu et al., 2008; Engling et al., 2006, 2009; Fine et al., 2001, 2004). We found that the Lev/Man ratios (Table 2) over the KCOG overlap between seasons and are somewhat close to those of hardwood burning emissions in northern China, Mongolia, and the Russian Far East, as corroborated by the backward air mass trajectories and MODIS fire counts (Figs. 1 and S1). Besides, Lev/ K^+ and Man/Gal ratios in summer differ from those of other seasons (Table 2). Cheng et al. (2013) have apportioned qualitatively the source contributions of anhydrosugars over a receptor site based on the comparison of Lev/ K^+ and Lev/Man ratios in aerosols to those from various source profiles compiled from the literature. This approach of using the mass ratios of Lev/Man and Lev/ K^+ has been proven useful for deciphering the difference in BB-derived OA (Bikkina et al., 2019).

Here, we adopted this methodology to ascertain the likely contributing sources of anhydrosugars, which are BB tracers from different seasons (Fig. 5). This source apportionment relies on the fact that the Lev/ K^+ ratio from the softwood burning (10–1000) is higher than from hardwood (1–100; Fine et al., 2004). In contrast, Lev/Man ratios for softwood are lower than those of hardwood burning (10–100; Fine et al., 2004). Likewise, the Lev/Man and Lev/ K^+ ratios from grasses and crop residues are 10–100 and 0.01–1.0, respectively (Bikkina et al., 2019). On a similar note,

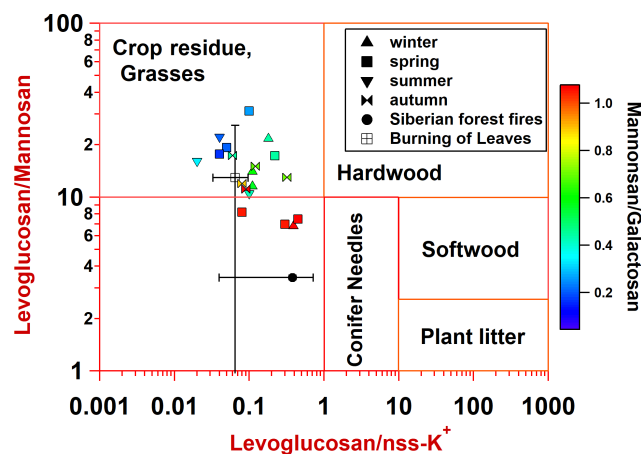


Figure 5. Scatterplot of levoglucosan/ K^+ (Lev/ K^+) versus levoglucosan/mannosan (Lev/Man) ratios in TSP collected over Gosan during April 2013–April 2014. The data for Siberian forest fires and burning leaves were adopted from Sullivan et al. (2008).

the Lev/ K^+ ratios from the burning of pine needles (0.1–1.0) somewhat overlap with those from hardwood burning emissions but are characterized by distinct Lev/Man ratios (Bikkina et al., 2019). The burning of dead leaves (duff) showed higher Lev/ K^+ ratios than those of pine needles and grasses, but their Lev/Man ratio is on the lower side than for the former biomass type and the softwood burning emissions. However, Lev is more susceptible to degradation by photooxidation with OH radicals during atmospheric transport (half-life of < 2.2 d; Hennigan et al., 2010), and this would cause lower abundances of this anhydrosugar. Hence, the hardwood Lev/ K^+ ratios could slightly shift downwards. Therefore, caution is required while interpreting the ambient data from a receptor site (Bikkina et al., 2019). Overlapping the seasonal data on this scatterplot of Lev/ K^+ versus Lev/Man (Fig. 5) clearly reveals a mixed contribution of the burning of hardwood and crop residue in the East Asian outflow. It should be noted that the photooxidation process during atmospheric transport is also applicable for low concentrations and poor correlations of other primary saccharides.

The correlation coefficients and diagnostic ratios of BSOA tracers specify their source origin or formation pathway. Nevertheless, the atmospheric stability or reactivity of BSOA tracers through the photooxidation during long-range transport may bias the correlation coefficients in Gosan aerosols. 2-MGA showed a significant correlation with 2-MTs ($r = 0.79$; $p < 0.01$) and C_5 -alkene triols ($r = 0.50$; $p < 0.05$; Fig. 6a, b), suggesting their similar formation pathway or common sources of isoprene SOA tracers. However, a poor correlation coefficient between 2-MTs and C_5 -alkene triols ($r = 0.33$; $p = 0.13$; Fig. 6c) indicates their different formation process over the Gosan atmosphere. Wang et al. (2005) documented that polyols are formed from isoprene through diepoxy derivatives, which further convert into 2-MTs by

Table 2. Statistical summary of diagnostic ratios and carbonaceous components contribution in Gosan aerosols.

| Species | Annual (avg. ^a ± SD ^b , min. ^c , max. ^d) | Summer (avg. ± SD, min., max.) | Fall (avg. ± SD, min., max.) | Winter (avg. ± SD, min., max.) | Spring (avg. ± SD, min., max.) |
|--|---|--------------------------------------|------------------------------------|--------------------------------------|--------------------------------------|
| Diagnostic ratios | | | | | |
| Lev/Man | 15.1 ± 6.76 6.81, 31.3 | 17.1 ± 8.21 8.58, 28.4 | 13.7 ± 2.51 11.1, 17.3 | 13.5 ± 6.24 6.81, 21.7 | 15.4 ± 8.76 6.98, 31.3 |
| Man/Gal | 0.55 ± 0.32 0.10, 1.07 | 0.28 ± 0.13 0.10, 0.42 | 0.64 ± 0.20 0.37, 0.90 | 0.66 ± 0.27 0.43, 1.05 | 0.61 ± 0.43 0.16, 1.07 |
| Lev/(Man + Gal) | 4.27 ± 1.23 2.18, 6.56 | 3.12 ± 0.78 2.18, 4.03 | 5.08 ± 0.32 4.71, 5.51 | 4.85 ± 1.35 3.49, 6.56 | 4.17 ± 1.33 2.50, 6.45 |
| Lev/K ⁺ × 10 ⁻² | 5.73 ± 5.65 0.65, 23.2 | 1.00 ± 0.52 0.65, 1.91 | 3.94 ± 2.51 1.26, 6.30 | 12.3 ± 7.87 6.42, 23.2 | 6.65 ± 4.48 1.77, 15.3 |
| Lev/OC × 10 ⁻² | 0.73 ± 0.66 0.08, 2.29 | 0.14 ± 0.10 0.08, 0.31 | 0.84 ± 0.61 0.12, 1.56 | 1.60 ± 0.67 0.99, 2.29 | 0.56 ± 0.40 0.11, 1.05 |
| Lev/WSOC × 10 ⁻² | 1.09 ± 0.97 0.10, 3.46 | 0.20 ± 0.13 0.10, 0.42 | 1.25 ± 0.94 0.23, 2.21 | 2.33 ± 0.90 1.48, 3.46 | 0.92 ± 0.65 0.13, 1.69 |
| 2-MGA/2-MLTs | 2.18 ± 1.59 0.33, 5.40 | 0.67 ± 0.43 0.33, 1.33 | 1.04 ± 0.49 0.41, 1.55 | 3.60 ± 1.43 1.90, 5.40 | 3.27 ± 1.17 1.60, 4.75 |
| ^e P/MBTCA | 0.62 ± 0.61 0.17, 5.90 | 3.22 ± 0.62 2.47, 3.89 | 3.62 ± 1.67 1.52, 5.90 | 1.68 ± 0.64 0.83, 2.38 | 1.73 ± 1.07 0.34, 3.32 |
| Carbonaceous components | | | | | |
| Isoprene-derived SOC (μg C m ⁻³) | 23.7 ± 23.9 2.26, 97.4 | 51.0 ± 32.4 8.08, 97.4 | 25.9 ± 17.9 8.54, 45.7 | 8.52 ± 1.07 7.46, 9.87 | 11.3 ± 6.80 2.26, 24.9 |
| Isoprene SOC to OC (%) | 1.45 ± 1.74 0.21, 6.40 | 3.56 ± 2.18 1.03, 6.40 | 1.46 ± 1.38 0.35, 3.48 | 0.35 ± 0.17 0.21, 0.57 | 0.57 ± 0.38 0.24, 1.35 |
| Isoprene SOC to total SOC (%) | 35.5 ± 15.5 13.5, 71.1 | 46.6 ± 20.3 26.0, 71.1 | 38.1 ± 10.4 21.1, 47.3 | 31.6 ± 7.05 24.0, 39.7 | 27.9 ± 15.5 13.5, 54.0 |
| Monoterpene SOC (μg C m ⁻³) | 40.1 ± 33.3 7.18, 154 | 62.7 ± 56.5 19.2, 154 | 40.7 ± 20.0 11.8, 57.7 | 19.3 ± 5.61 14.0, 25.2 | 35.5 ± 23.5 7.18, 62.7 |
| Monoterpene SOC to OC (%) | 2.0 ± 1.47 0.37, 5.74 | 3.65 ± 1.58 2.44, 5.74 | 2.15 ± 1.45 0.48, 3.88 | 0.87 ± 0.58 0.37, 1.48 | 1.58 ± 0.84 0.54, 3.13 |
| Monoterpene SOC to total SOC (%) | 64.5 ± 15.5 28.9, 86.5 | 53.4 ± 20.3 28.9, 74.0 | 61.9 ± 10.4 52.7, 78.9 | 68.4 ± 7.05 60.3, 76.1 | 72.1 ± 15.5 46.0, 86.5 |

^a Average, ^b standard deviation, ^c minimum, and ^d maximum. ^e P is *cis*-pinonic acid and pinic acid.

acid-catalyzed hydrolysis. On the other hand, C₅-alkene triols are produced from the precursor of hydroxyperoxy radicals that are initially derived from isoprene through rearrangement reactions (Surratt et al., 2006). It can be noted that the formation mechanisms of 2-MGA and 2-MTs are different while depending on the NO_x concentrations (Surratt et al., 2010). Thus, the ratio of 2-MGA/2-MTs attributes to the influence of NO_x on isoprene SOA formation. We found a low ratio of 2-MGA/2-MTs (0.67; Fig. S5a in the Supplement; Table 2) in summer, implying the enhancement of 2-MTs formation over the open ocean due to the low NO_x environment in the ocean atmosphere. On the contrary, the 2-MGA/2-MTs ratios for other seasons were > 1.0 (Fig. S5a; Table 2), indicating an elevated formation of 2-MGA through the continental high NO_x condition, which is consistent with the air masses back trajectory.

Cis-pinonic acid showed a weak correlation with pinic acid ($r = 0.35$; $p = 0.12$; Fig. 6f), suggesting that different atmospheric reactivity of *cis*-pinonic/pinic acids during transport would cause such poor correlation. In contrast, pinic acid exhibited a strong positive linear correlation with 3-HGA ($r = 0.90$; $p < 0.01$) and MBTCA ($r = 0.90$; $p < 0.01$; Fig. 6d, e), implying their similar sources. It should be noted that the formation processes of pinic acid, 3-HGA, and MBTCA are different because pinic acid is a first-generation product, and 3-HGA and MBTCA are high-generation products (Claeys et al., 2007; Müller et al., 2012; Szmigielski et al., 2007). The ratio of *cis*-pinonic acid + pinic acid to MBTCA (P/M) is used to evaluate the aging of monoterpene SOA.

A low P/M ratio suggests the transformation of *cis*-pinonic and pinic acids to MBTCA and, thus, relatively aged

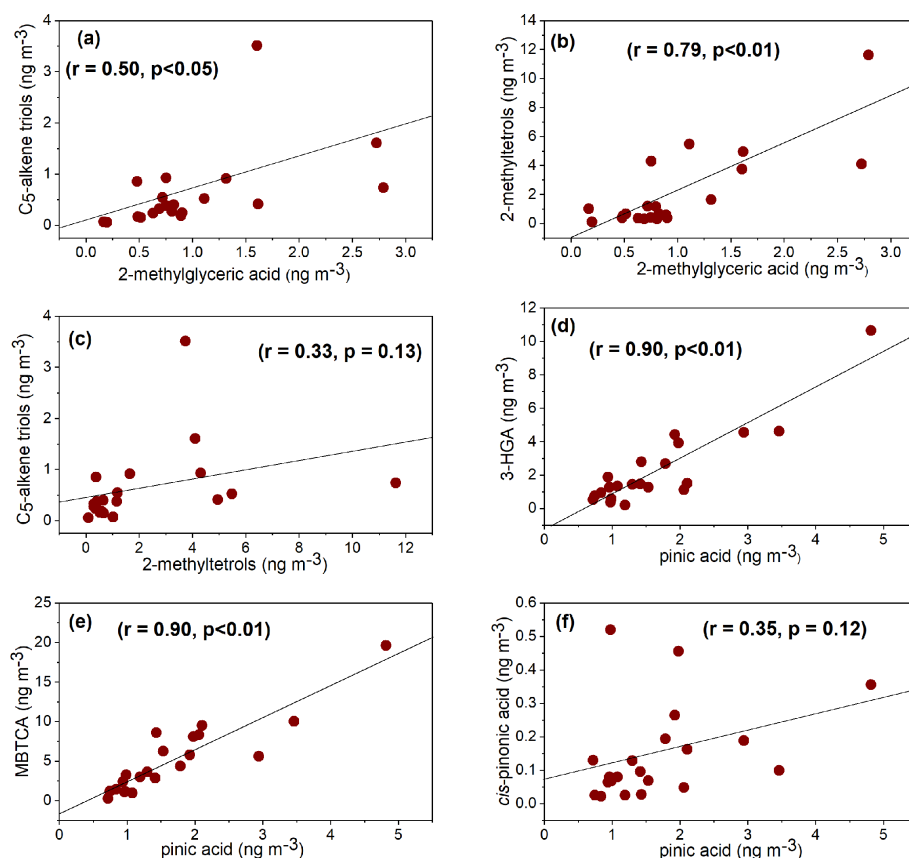


Figure 6. Pearson linear correlation coefficient analysis of BSOA tracers in Gosan TSP aerosols during April 2013–April 2014.

monoterpene SOA, whereas a high ratio reflects relatively fresh monoterpene SOA (Gómez-González et al., 2012; Ding et al., 2014). Gómez-González et al. (2012) reported aged monoterpene SOA ($P/M = 0.84$) from a Belgian forest site, while fresh chamber-produced α -pinene SOA tracers showed P/M ratios of 1.51 to 3.21 (Offenberg et al., 2007). The average ratio of P/M in this study was 0.62, with the low value in summer (Fig. S5b; Table 2), which is lower than those of Guangzhou (fresh monoterpene SOA; 28.9) while the air masses originated from southern China (Ding et al., 2014). This observation indicates that monoterpenes SOA have undergone substantial aging during transport to Gosan, particularly in summer when extensive photochemical oxidation occurred due to the high temperature and intense solar radiation.

3.5 Relative abundances in WSOC and OC

Levoglucosan is the most abundant anhydrosugar, contributing 0.05 %–1.54 % of WSOC and 0.03 %–1.02 % of OC. Likewise, sucrose, glucose, and fructose were more abundant primary sugars, contributing 0.01 %–2.83 %, 0.03 %–1.22 %, and 0.02 %–0.74 % of WSOC, respectively. Contributions of the three primary sugars varied from 0.05 % to 3.41 % of OC.

Arabitol and mannitol are the most abundant sugar alcohols, whose contribution to WSOC and OC ranged from 0.02 % and 0.93 % to 0.01 % and 0.85 %, respectively. Figure 7 depicts the contribution of sugar compounds to WSOC and OC in TSP collected over Gosan during the study period. We also compared the atmospheric abundances of sugar compounds from Gosan with the literature data (Table 3). This comparison revealed the lesser influence of BB tracer compounds (i.e., anhydrosugar levels) over Gosan, which is a factor of 5–10 times lower than those reported for the BB-influenced source regions in China and East Asia (P. Q. Fu et al., 2012; Kang et al., 2018a; Wang and Kawamura, 2005; Wang et al., 2012). However, the levels of anhydrosugar over Gosan are higher than those observed over the remote Canadian High Arctic research site (Fu et al., 2009a). In contrast, Gosan is characterized by high concentrations of primary sugars compared to other remote sampling sites in Table 3. This is because of the overwhelming contribution of primary sugars associated with soil dust particles over Gosan during the East Asian outflow. Such high loadings of primary sugars were observed from other remote island receptor sites in the WNP (Okinawa) during the spring season (Zhu et al., 2015a). Likewise, the concentrations of sugar alcohols from Gosan are

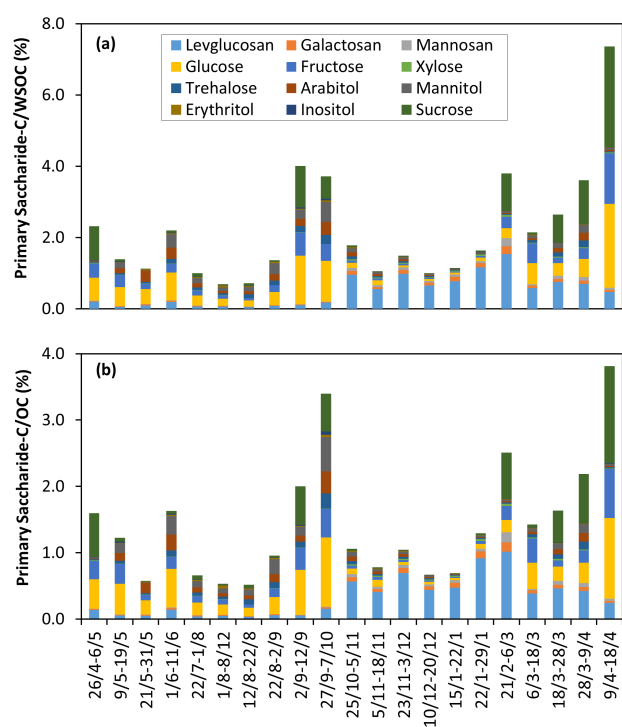


Figure 7. Contribution of primary saccharide C in (a) WSOC (percent), and (b) OC (percent) in TSP collected over Gosan during April 2013–April 2014.

similar to those from other receptor sites influenced by the East Asian outflow (Verma et al., 2018; Zhu et al., 2015a).

The contributions of isoprene SOA tracers to ambient OC (0.01 %–0.40 %; avg. 0.09 %) and WSOC (0.02 %–0.57 %; avg. 0.13 %) were lower than those of monoterpene-derived SOA (0.04 %–0.63 % and avg. 0.23 % for OC and 0.06 %–0.82 % and avg. 0.33 % for WSOC). The contributions of isoprene oxidation products to OC and WSOC were found to be highest in summer (0.23 % and 0.32 %, respectively), followed by fall (0.09 % and 0.13 %), spring (0.04 % and 0.06 %), and winter (0.02 % and 0.03 %). Likewise, the contributions of monoterpene SOA products to aerosol OC and WSOC exhibited the highest value in summer (0.40 % and 0.55 %, respectively), followed by fall (0.24 % and 0.35 %), spring (0.18 % and 0.27 %), and winter (0.10 % and 0.14 %). We found that the contribution of BSOA products to the carbonaceous components occurred twice in summer (Fig. 8, Table 2). This means BSOA formation occurred to a greater extent in summer due to the intensive BVOCs emission with key factors of meteorological parameters (higher temperature and radiation), i.e., higher concentrations of ozone, and other oxidizing agents (NO_x , OH, etc.). It should be pointed out that the fraction of WSOC in OC (WSOC/OC) is often prone to photochemical aging and, hence, contributes to SOA. More specifically, the WSOC/OC > 0.4 over a receptor site indicates aged aerosols with a significant SOA con-

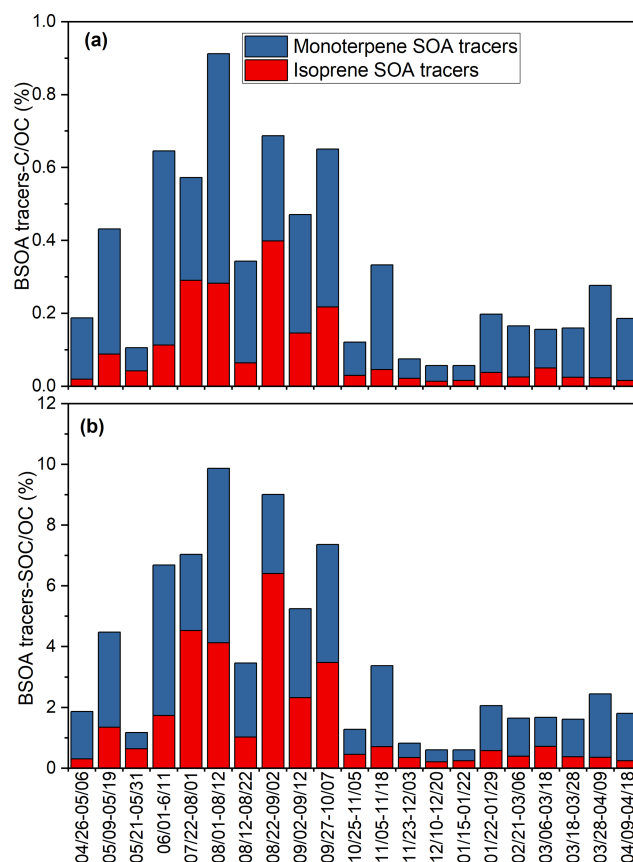


Figure 8. Contribution of (a) isoprene and monoterpene SOA tracers of C in ambient OC (percent) and (b) isoprene and monoterpene SOA tracers SOC in ambient OC (percent) in Gosan aerosol samples during April 2013–April 2014.

tribution (Haque et al., 2019; Boreddy et al., 2018). In our study, the average WSOC/OC ratio observed was 0.68, with the highest ratio in summer (0.72), although a subtle difference existed in winter/fall (> 0.68), implying the presence of aged OA over the KCOG. Such higher abundances of SOA over Gosan during transport from East Asia is mainly due to photochemical aging of anthropogenic (fossil fuel/biomass combustion) emissions. Huang et al. (2014) reported significant SOA formation from the fossil fuel/biomass combustion precursor VOCs in winter over China.

We estimated secondary organic carbon (SOC), derived from isoprene and monoterpenes, using the measured values of BSOA tracers and following the SOA-tracer-based method first proposed by Kleindienst et al. (2007). A summary of the estimated SOC is provided in Table 2. The contribution of isoprene to SOC was calculated as being from 2.26 to 97.4 ng C m^{-3} (avg. 23.7 ng C m^{-3}), accounting for 1.45 % of OC and 35.5 % of total biogenic SOC, with the predominance in summer (3.56 % and 46.6 % for OC and SOC, respectively). The estimation of monoterpene SOA to SOC (avg. 40.1 ng C m^{-3}) was observed to be around 2 times

Table 3. Comparisons of the mean concentration (ng m^{-3}) of anhydrosugars, sugar, and sugar alcohols in Gosan aerosols with those from different sites around the world.

| Sampling sites | Sampling type | Sampling time | Anhydro-sugars | Primary sugars | Sugar alcohols | References |
|-----------------------------------|-------------------|---------------|----------------|----------------|----------------|---------------------------|
| Gosan, South Korea | TSP | Summer | 3.74 | 22.8 | 14.3 | This study |
| | | Fall | 25.9 | 38.3 | 13.4 | |
| | | Winter | 48.0 | 20.2 | 2.60 | |
| | | Spring | 15.7 | 90.0 | 7.36 | |
| Chennai, India | PM ₁₀ | Summer | 127 | 15.5 | 7.44 | P. Q. Fu et al. (2010) |
| | | Winter | 134 | 11.4 | 4.81 | |
| Mt. Tai, China | TSP | Summer (June) | 224 | 61.1 | 125 | P. Q. Fu et al. (2012) |
| Alert, Canada | TSP | Winter | 0.32 | 1.14 | 0.25 | Fu et al. (2009a) |
| | | Spring | 0.02 | 0.18 | 0.36 | |
| Okinawa, western North Pacific | TSP | Summer | 0.93 | 73.5 | 62.9 | Zhu et al. (2015a, b) |
| | | Fall | 2.58 | 56.0 | 30.7 | |
| | | Winter | 6.04 | 34.4 | 6.03 | |
| | | Spring | 3.44 | 101 | 31.2 | |
| Chichijima, western North Pacific | TSP | Summer | 0.32 | 32.8 | 38.6 | Verma et al. (2015, 2018) |
| | | Fall | 0.85 | 22.0 | 35.1 | |
| | | Winter | 2.40 | 14.2 | 3.93 | |
| | | Spring | 0.94 | 24.2 | 15.5 | |
| Mt. Hua, China (non-dust storm) | PM ₁₀ | April | 57.8 | 92.5 | 22.4 | Wang et al. (2012) |
| Mt. Hua, China (dust storm) | PM ₁₀ | April | 44.5 | 162 | 25.7 | Wang et al. (2012) |
| Nanjing, China | PM _{2.5} | Summer | 151 (Lev) | 59.3 | 11.8 | Wang and Kawamura (2005) |
| | | Winter | 268 (Lev) | 42.3 | 13.4 | |
| Beijing, China | PM _{2.5} | Summer | 14.5 | 6.63 | 3.31 | Kang et al. (2018a) |
| | | Fall | 129 | 17.2 | 13.7 | |
| | | Winter | 254 | 41.5 | 17.8 | |
| | | Spring | 81.4 | 33.9 | 12.3 | |
| Belgrade, Serbia | TSP | Fall | 425 (Lev) | 116 | 98.4 | Zangrado et al. (2016) |
| Maine, USA | PM ₁ | May–October | 13.9 | 28 | 8.31 | Medeiros et al. (2006) |
| Crete, Greece | PM ₁₀ | Year round | 14.4 | 32.3 | 6.53 | Theodosi et al. (2018) |

higher than that of isoprene SOA (Table 2). Interestingly, the contribution of monoterpene-derived SOC to ambient OC (3.65 %) was dominant in summer, but monoterpene SOC to total SOC (72.1 %) was most abundant in spring (Fig. 8b). The seasonal distributions of biogenic SOC (Table 2) imply that a substantial amount of SOC was formed from monoterpenes in spring. The estimated biogenic SOC at the KCOG is almost 1 order of magnitude lower than that from other continental sites in Chinese urban areas (e.g., Pearl River Delta is 446 ng C m^{-3} ; Ding et al., 2012). However, the estimated biogenic SOC load from the KCOG is much higher than that reported from a remote site in the Canadian High Arctic (Alert is 9.4 ng C m^{-3} ; Fu et al., 2009b) and is comparable with that over the East China Sea (Kang et al., 2018b).

It should be noted that concentrations of SOA tracers cannot always provide the actual contribution of the biogenic source to ambient organic aerosol mass. For example, loadings of monoterpene SOA tracers were lower in sample KOS999 (28 March–9 April 2014; 3.02 ng m^{-3}) compared to sample KOS1000 (9–18 April 2014; 14.4 ng m^{-3}), whereas the estimated contribution of SOC to ambient OC showed an opposite trend (KOS999 is 2.08 %; KOS1000 is 1.56 %). This result demonstrates that the estimation of SOC is an important factor in evaluating the contribution of BSOA to organic aerosol mass. We calculated biogenic OC using radiocarbon (^{14}C) data following the method proposed by Szidat et al. (2006). Biogenic OC showed a poor correlation with biogenic SOC ($r = 0.36$; $p = 0.09$) but a significant

linear relationship with primary sugars (i.e., glucose, fructose, and sucrose; $r = 0.54$; $p < 0.5$), suggesting that primary bioaerosols from plant-derived airborne pollen dictate biogenic OC over Gosan.

3.6 Significance of fossil fuel as a source for levoglucosan

The ambient Lev levels showed a significant linear relationship with the $\text{OC}_{\text{fossil}}$, suggesting the fossil source contribution of this molecular marker (Fig. 9a). However, such a significant correlation was not evident between $\text{OC}_{\text{fossil}}$ and other major sugar compounds. Until recently, Lev has been thought to originate primarily from the hemicellulose/cellulose pyrolysis of vegetation and, hence, can be employed as a powerful tracer for biomass smoke particles (Fraser and Lakshmanan, 2000; Simoneit et al., 1999). Nevertheless, residential coals (e.g., lignite and bituminous coal) have been shown to contain high concentrations of Lev but also emit traces of Man and Gal (Kourtev et al., 2011; Fabri et al., 2008). Recently, Yan et al. (2018) found a significant linear relationship between the ^{14}C -based fossil fraction of WSOC and Lev C in the aerosols generated from coal combustion and the ambient aerosol samples. Therefore, the prevailing linear relationship between $\text{OC}_{\text{fossil}}$ and Lev C in the Gosan samples (Fig. 9a) is likely due to a common source contribution from coal combustion in East Asia.

The slope of the linear regression between Lev C and $\text{OC}_{\text{fossil}}$ (0.0094; Fig. 9a) is higher than those documented for the coal combustion source in China ($\sim 0.004 \pm 0.007$; Yan et al., 2018). Moreover, Lev C moderately correlated with the $\text{EC}_{\text{fossil}}$, with the regression slope (~ 0.01) in the Gosan samples (Fig. 9b), thus being comparable to that observed for the coal combustion in China (0.044 ± 0.076 ; Yan et al., 2018). It should be noted that when excluding the three outliers as shown in Fig. 9b (black square), Lev C showed a stronger correlation with $\text{EC}_{\text{fossil}}$ ($R^2 = 0.74$; $p < 0.05$). Of these, two outliers in winter (KOS995 is 22–29 January 2014; KOS996 is 21 February–3 March 2014) have higher Lev C levels over that of $\text{EC}_{\text{fossil}}$ when air mass trajectories showed the impact of BB emissions in the North China Plain. In contrast, the third outlier in summer (KOS979 is 1–11 June 2013) has a lower Lev C/ $\text{EC}_{\text{fossil}}$, while air parcels transported from nearby cities in China, Korea, and Japan, thus, have more contributions from vehicular emissions. Overall, both regression slopes are, thus, the representative nature of Lev C/ $\text{OC}_{\text{fossil}}$ and Lev C/ $\text{EC}_{\text{fossil}}$ in the East Asian outflow. Lev C and nss SO_4^{2-} exhibited a poor correlation (Fig. 9c), although both were transported from East Asia.

Lev C exhibited a rather weaker correlation with $\text{OC}_{\text{nonfossil}}$ ($R^2 = 0.19$) than with $\text{EC}_{\text{nonfossil}}$ ($R^2 = 0.42$) over Gosan during the study period (Fig. 9d, e). This could be likely because $\text{OC}_{\text{nonfossil}}$ has contributions from the BB and the secondary formation process or the primary biogenic sources. The contribution of primary OC generated from BB

(POC_{BB}) to $\text{OC}_{\text{nonfossil}}$ was taken from Zhang et al. (2016). In their study, the ^{14}C -based $\text{EC}_{\text{nonfossil}}$ levels were scaled by a factor to constrain the POC_{BB} (Zhang et al., 2016). Here the conversion factor is 4.5 (range of 3–10), which is a median value representing the primary OC/EC ratio from BB emissions ($(\text{POC}/\text{EC})_{\text{BB}}$).

$$\text{POC}_{\text{BB}} = \text{EC}_{\text{nonfossil}} \times (\text{POC}/\text{EC})_{\text{BB}}. \quad (7)$$

Lev C showed a somewhat improved linear correlation with POC_{BB} than with $\text{OC}_{\text{nonfossil}}$ (Fig. 9f). It is apparent from Fig. 9 that the regression slopes are comparable, indicating the contribution to Lev from both coal combustion and BB emissions over Gosan. The prevailing weak linear relationship (moderate correlation) of Lev with nonfossil and fossil carbon fractions is likely the result of photodegradation of Lev during atmospheric transport. This result would mean that the higher atmospheric abundance of Lev and its pronounced linear relationships with the nonfossil and fossil carbon fractions imply a much stronger impact of both source emissions in East Asia during the continental outflow in winter and spring.

Overall, we present a new finding on the contribution of coal combustion sources in East Asia in controlling the atmospheric levels of Lev apart from the traditional biomass/biofuel burning emissions. This is based on the prevailing linear relationship between the radiocarbon-based nonfossil EC and Lev in the year-round TSP samples collected from the KCOG site in Jeju Island. The Gosan supersite is the best location to understand how the chemical composition of source emissions from East Asia affects the outflow regions in winter and spring. Recent studies have highlighted the potential contribution of Lev from residential coal combustion in China (Yan et al., 2018), with an estimated annual emission of $\sim 2.2 \text{ Gg}$ of Lev from domestic coal combustion (Wu et al., 2021). Given this background information, the prevailing significant linear relationship between Lev and nonfossil EC (p value < 0.05) over the KCOG clearly emphasizes the need for a reconsideration of the previous assessments on the impact of BB in East Asian outflow to the WNP. Additionally, this dataset is further compared with the molecular distributions and relative abundances of organic tracers in the TSP samples collected over Gosan during 2001, which is a decade ago (P. Fu et al., 2012). This comparison allows us to better understand the regional changes in the emission sources (e.g., fugitive dust, BB, and fossil fuel combustion) on a decadal basis.

4 Conclusions

We investigated seasonal variations in primary organic components such as anhydrosugars, primary sugars, sugar alcohols, and BSOA tracers (isoprene- and monoterpene-derived SOA products) in ambient aerosols from Gosan on Jeju Island. Among the detected sugar compounds, levoglucosan

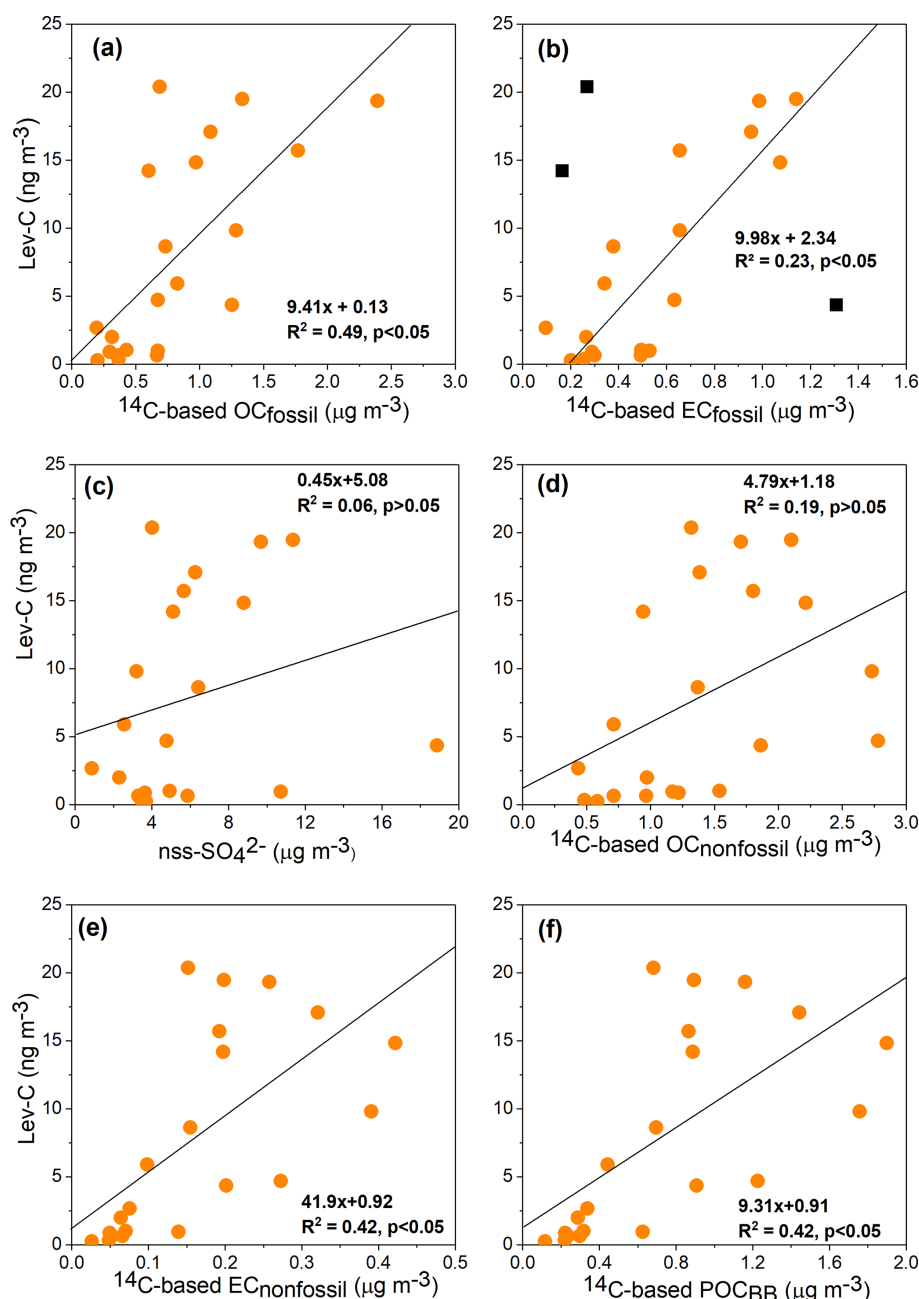


Figure 9. Linear regression analysis between levoglucosan in terms of its carbon content (Lev C) and ^{14}C -based mass concentrations of (a) organic carbon and (b) elemental carbon of fossil origin ($\text{OC}_{\text{fossil}}$ and $\text{EC}_{\text{fossil}}$, respectively). (c) Values of nss SO_4^{2-} , (d) nonfossil-derived organic carbon ($\text{OC}_{\text{nonfossil}}$), (e) nonfossil-derived elemental carbon ($\text{EC}_{\text{nonfossil}}$), and (f) biomass-burning-derived primary OC (POC_{BB}) in TSP collected over Gosan during April 2013–April 2014. In panel (b), the squares represent three outliers (i.e., samples with rather high and low Lev/EC ratios; please see the text for more details).

was dominant in winter/fall, whereas glucose and sucrose were more abundant in spring/summer. The seasonal trends documented that the BB impact is more significant in winter/fall and the primary bioaerosol particles are important in spring/summer. Diagnostic ratios of levoglucosan, galactosan, and mannosan reflect that emissions from BB are mostly dominated by hardwood. The significant linear rela-

tionship of sucrose with glucose and fructose suggests their origin from airborne pollen. On a similar note, trehalose showed a significant positive correlation with arabinol, mannitol, and erythritol, implying their contribution from airborne fungal spores and soil microbes over the KCOG.

Distributions of biogenic SOA tracers were characterized by a predominance of monoterpene-derived than isoprene-

derived oxidation products in Gosan aerosols. The BSOA tracers were formed in summer to a greater extent, followed by fall/spring and then winter. The low ratio of *cis*-pinonic acid + pinic acid to MBTCA demonstrated that monoterpene SOA was relatively aged over Gosan aerosols. The estimated SOC with the predominance in summer shows that substantial BSOA formation occurred in summer due to favorable meteorological conditions. The backward air mass trajectories and source apportionment studies entirely demonstrated that emission from East Asia significantly dominates the ambient OA mass over KCOG. Interestingly, levoglucosan C exhibited a significant positive correlation with nonfossil and fossil organic carbon fractions, along with the comparable regression slopes. This result reveals that BB and coal (lignite) combustion both are prominent sources for levoglucosan in the East Asian outflow.

Although there is some evidence that levoglucosan could originate from the combustion of brown coals (e.g., lignite) in China, our observations from the KCOG (receptor site) also hint at the fossil source contribution of this molecular marker in the regional influx of the East Asian outflow. Therefore, the attribution of ambient levoglucosan levels over the WNP to the impact of BB emission may cause large uncertainty.

Data availability. The data used in this paper are available upon request from the corresponding author.

Supplement. The supplement related to this article is available online at: <https://doi.org/10.5194/acp-22-1373-2022-supplement>.

Author contributions. KK and YZ designed the research. ML collected the aerosol samples. MMH and SB performed the analysis of aerosol samples. MMH wrote the paper under the guidance of YZ and KK. All authors were actively involved in the discussion of the paper.

Competing interests. At least one of the (co-)authors is a member of the editorial board of *Atmospheric Chemistry and Physics*. The peer-review process was guided by an independent editor, and the authors also have no other competing interests to declare.

Disclaimer. Publisher's note: Copernicus Publications remains neutral with regard to jurisdictional claims in published maps and institutional affiliations.

Acknowledgements. We acknowledge the financial supports of the Japan Society for the Promotion of Science (JSPS; grant no. 24221001) and the National Natural Science Foundation of China (grant No. 41977305).

Financial support. This research has been supported by the National Natural Science Foundation of China (grant no. 41977305) and the Japan Society for the Promotion of Science (grant no. 24221001).

Review statement. This paper was edited by Willy Maenhaut and reviewed by two anonymous referees.

References

- Arimoto, R., Duce, R. A., Savoie, D. L., Prospero, J. M., Talbot, R., Cullen, J. D., Tomza, U., Lewis, N. F., and Ray, B. J.: Relationships among aerosol constituents from Asia and the North Pacific during PEM-West A, *J. Geophys. Res.-Atmos.*, 101, 2011–2023, <https://doi.org/10.1029/95JD01071>, 1996.
- Bauer, H., Claeys, M., Vermeylen, R., Schueller, E., Weinke, G., Berger, A., and Puxbaum, H.: Arabitol and mannitol as tracers for the quantification of airborne fungal spores, *Atmos. Environ.*, 42, 588–593, 2008.
- Bikkina, S., Haque, M. M., Sarin, M., and Kawamura, K.: Tracing the relative significance of primary versus secondary organic aerosols from biomass burning plumes over coastal ocean using sugar compounds and stable carbon isotopes, *ACS Earth Space Chem.*, 3, 1471–1484, <https://doi.org/10.1021/acsearthspacechem.9b00140>, 2019.
- Bikkina, S., Kawamura, K., Sakamoto, Y., and Hirokawa, J.: Low molecular weight dicarboxylic acids, oxocarboxylic acids and α -dicarbonyls as ozonolysis products of isoprene: Implication for the gaseous-phase formation of secondary organic aerosols, *Sci. Total Environ.*, 769, 144472, <https://doi.org/10.1016/j.scitotenv.2020.144472>, 2021.
- Birch, M. E. and Cary, R. A.: Elemental carbon-based method for monitoring occupational exposures to particulate diesel exhaust, *Aerosol Sci. Tech.*, 25, 221–241, 1996.
- Boreddy, S. K. R., Haque, M. M., and Kawamura, K.: Long-term (2001–2012) trends of carbonaceous aerosols from a remote island in the western North Pacific: an outflow region of Asian pollutants, *Atmos. Chem. Phys.*, 18, 1291–1306, <https://doi.org/10.5194/acp-18-1291-2018>, 2018.
- Broadgate, W. J., Liss, P. S., and Penkett, S. A.: Seasonal emissions of isoprene and other reactive hydrocarbon gases from the ocean, *Geophys. Res. Lett.*, 24, 2675–2678, <https://doi.org/10.1029/97GL02736>, 1997.
- Cheng, Y., Engling, G., He, K.-B., Duan, F.-K., Ma, Y.-L., Du, Z.-Y., Liu, J.-M., Zheng, M., and Weber, R. J.: Biomass burning contribution to Beijing aerosol, *Atmos. Chem. Phys.*, 13, 7765–7781, <https://doi.org/10.5194/acp-13-7765-2013>, 2013.
- Claeys, M., Graham, B., Vas, G., Wang, W., Vermeylen, R., Pashynska, V., Cafmeyer, J., Guyon, P., Andreae, M. O., Artaxo, P., and Maenhaut, W.: Formation of secondary organic aerosols through photooxidation of isoprene, *Science*, 303, 1173–1176, 2004.
- Claeys, M., Szmigielski, R., Kourtchev, I., van der Veken, P., Vermeylen, R., Maenhaut, W., Jaoui, M., Kleindienst, T. E., Lewandowski, M., Offenberg, J., and Edney, E. O.: Hydroxydicarboxylic acids: Markers for secondary organic aerosol from the photooxidation of α -pinene, *Environ. Sci. Technol.*, 41, 1628–1634, 2007.

- Conte, L., Szopa, S., Aumont, O., Gros, V., and Bopp, L.: Sources and sinks of isoprene in the global open ocean: Simulated patterns and emissions to the atmosphere, *J. Geophys. Res.-Oceans*, 9, e2019JC015946, <https://doi.org/10.1029/2019JC015946>, 2020.
- Deguille, L., Leriche, M., Amato, P., Ariya, P. A., Delort, A.-M., Pöschl, U., Chaumerliac, N., Bauer, H., Flossmann, A. I., and Morris, C. E.: Microbiology and atmospheric processes: chemical interactions of primary biological aerosols, *Biogeosciences*, 5, 1073–1084, <https://doi.org/10.5194/bg-5-1073-2008>, 2008.
- Ding, X., Wang, X. M., Gao, B., Fu, X. X., He, Q. F., Zhao, X. Y., Yu, J. Z., and Zheng, M.: Tracer-based estimation of secondary organic carbon in the Pearl River Delta, south China, *J. Geophys. Res.-Atmos.*, 117, D05313, <https://doi.org/10.1029/2011JD016596>, 2012.
- Ding, X., He, Q. F., Shen, R. Q., Yu, Q. Q., and Wang, X. M.: Spatial distributions of secondary organic aerosols from isoprene, monoterpenes, β -caryophyllene, and aromatics over China during summer, *J. Geophys. Res.*, 119, 11877–11891, <https://doi.org/10.1002/2014JD021748>, 2014.
- Engling, G., Carrico, C. M., Krelidenweis, S. M., Collett, J. L., Day, D. E., Malm, W. C., Lincoln, E., Hao, W. M., Iinuma, Y., and Herrmann, H.: Determination of levoglucosan in biomass combustion aerosol by high-performance anion-exchange chromatography with pulsed amperometric detection, *Atmos. Environ.*, 40, S299–S311, 2006.
- Engling, G., Lee, J. J., Tsai, Y. W., Lung, S. C. C., Chou, C. C. K., and Chan, C. Y.: Size-resolved anhydrosugar composition in smoke aerosol from controlled field burning of rice straw, *Aerosol Sci. Tech.*, 43, 662–672, <https://doi.org/10.1080/02786820902825113>, 2009.
- Fabbri, D., Marynowski, L., Fabianska, M. J., Zaton, M., and Simoneit, B. R. T.: Levoglucosan and other cellulose markers in pyrolysates of miocene lignites: Geochemical and environmental implications, *Environ. Sci. Technol.*, 42, 2957–2963, <https://doi.org/10.1021/Es7021472>, 2008.
- Fine, P. M., Cass, G. R., and Simoneit, B. R. T.: Chemical characterization of fine particle emissions from fireplace combustion of woods grown in the northeastern United States, *Environ. Sci. Technol.*, 35, 2665–2675, 2001.
- Fine, P. M., Cass, G. R., and Simoneit, B. R. T.: Chemical characterization of fine particle emissions from the fireplace combustion of wood types grown in the Midwestern and Western United States, *Environ. Eng. Sci.*, 21, 387–409, 2004.
- Fraser, M. P. and Lakshmanan, K.: Using levoglucosan as a molecular marker for the long-range transport of biomass combustion aerosols, *Environ. Sci. Technol.*, 34, 4560–4564, <https://doi.org/10.1021/es991229l>, 2000.
- Fu, P., Kawamura, K., Kanaya, Y., and Wang, Z.: Contributions of biogenic volatile organic compounds to the formation of secondary organic aerosols over Mt. Tai, Central East China, *Atmos. Environ.*, 44, 4817–4826, <https://doi.org/10.1016/j.atmosenv.2010.08.040>, 2010.
- Fu, P., Kawamura, K., Kobayashi, M., and Simoneit, B. R. T.: Seasonal variations of sugars in atmospheric particulate matter from Gosan, Jeju Island: Significant contributions of airborne pollen and Asian dust in spring, *Atmos. Environ.*, 55, 234–239, <https://doi.org/10.1016/j.atmosenv.2012.02.061>, 2012.
- Fu, P. Q., Kawamura, K., Okuzawa, K., Aggarwal, S. G., Wang, G., Kanaya, Y., and Wang, Z.: Organic molecular compositions and temporal variations of summertime mountain aerosols over Mt. Tai, North China Plain, *J. Geophys. Res.-Atmos.*, 113, D1910, <https://doi.org/10.1029/2008JD009900>, 2008.
- Fu, P. Q., Kawamura, K., and Barrie, L. A.: Photochemical and other sources of organic compounds in the Canadian high Arctic aerosol pollution during winter-spring, *Environ. Sci. Technol.*, 43, 286–292, 2009a.
- Fu, P. Q., Kawamura, K., Chen, J., and Barrie, L. A.: Isoprene, monoterpene, and sesquiterpene oxidation products in the high Arctic aerosols during late winter to early summer, *Environ. Sci. Technol.*, 43, 4022–4028, 2009b.
- Fu, P. Q., Kawamura, K., Pavuluri, C. M., Swaminathan, T., and Chen, J.: Molecular characterization of urban organic aerosol in tropical India: contributions of primary emissions and secondary photooxidation, *Atmos. Chem. Phys.*, 10, 2663–2689, <https://doi.org/10.5194/acp-10-2663-2010>, 2010.
- Fu, P. Q., Kawamura, K., and Miura, K.: Molecular characterization of marine organic aerosols collected during a round-the-world cruise, *J. Geophys. Res.*, 116, D13302, <https://doi.org/10.1029/2011jd015604>, 2011.
- Fu, P. Q., Kawamura, K., Chen, J., Li, J., Sun, Y. L., Liu, Y., Tachibana, E., Aggarwal, S. G., Okuzawa, K., Tanimoto, H., Kanaya, Y., and Wang, Z. F.: Diurnal variations of organic molecular tracers and stable carbon isotopic composition in atmospheric aerosols over Mt. Tai in the North China Plain: an influence of biomass burning, *Atmos. Chem. Phys.*, 12, 8359–8375, <https://doi.org/10.5194/acp-12-8359-2012>, 2012.
- Gómez-González, Y., Wang, W., Vermeylen, R., Chi, X., Neirynck, J., Janssens, I. A., Maenhaut, W., and Claeys, M.: Chemical characterisation of atmospheric aerosols during a 2007 summer field campaign at Brasschaat, Belgium: sources and source processes of biogenic secondary organic aerosol, *Atmos. Chem. Phys.*, 12, 125–138, <https://doi.org/10.5194/acp-12-125-2012>, 2012.
- Graham, B., Guyon, P., Taylor, P. E., Artaxo, P., Maenhaut, W., Glovsky, M. M., Flagan, R. C., and Andreae, M. O.: Organic compounds present in the natural Amazonian aerosol: Characterization by gas chromatography-mass spectrometry, *J. Geophys. Res.-Atmos.*, 108, D24, 4766, <https://doi.org/10.1029/2003JD003990>, 2003.
- Griffin, R. J., Cocker, D. R., Seinfeld, J. H., and Dabdub, D.: Estimate of global atmospheric organic aerosol from oxidation of biogenic hydrocarbons, *Geophys. Res. Lett.*, 26, 2721–2724, 1999.
- Guenther, A., Hewitt, C. N., Erickson, D., Fall, R., Geron, C., Graedel, T., Harley, P., Klinger, L., Lerdau, M., McKay, W. A., Pierce, T., Scholes, B. R. S., Tallamraju, R., Taylor, J., and Zimmerman, P.: A global model of natural volatile organic compound emissions, *J. Geophys. Res.*, 100, 8873–8892, 1995.
- Guenther, A., Karl, T., Harley, P., Wiedinmyer, C., Palmer, P. I., and Geron, C.: Estimates of global terrestrial isoprene emissions using MEGAN (Model of Emissions of Gases and Aerosols from Nature), *Atmos. Chem. Phys.*, 6, 3181–3210, 2006.
- Haque, Md. M., Kawamura, K., Deshmukh, D. K., Fang, C., Song, W., Mengying, B., and Zhang, Y.-L.: Characterization of organic aerosols from a Chinese megacity during winter: pre-

- dominance of fossil fuel combustion, *Atmos. Chem. Phys.*, 19, 5147–5164, <https://doi.org/10.5194/acp-19-5147-2019>, 2019.
- Heald, C. L. and Spracklen, D. V.: Atmospheric budget of primary biological aerosol particles from fungal spores, *Geophys. Res. Lett.*, 36, L09806, <https://doi.org/10.1029/2009GL037493>, 2009.
- Heald, C. L., Henze, D. K., Horowitz, L. W., Feddes, J., Lamarque, J. F., Guenther, A., Hess, P. G., Vitt, F., Seinfeld, J. H., Goldstein, A. H., and Fung, I.: Predicted change in global secondary organic aerosol concentrations in response to future climate, emissions, and land use change, *J. Geophys. Res.*, 113, D05211, <https://doi.org/10.1029/2007jd009092>, 2008.
- Hennigan, C. J., Sullivan, A. P., Collett, J. L., and Robinson, A. L.: Levoglucosan stability in biomass burning particles exposed to hydroxyl radicals, *Geophys. Res. Lett.*, 37, L09806, <https://doi.org/10.1029/2010GL043088>, 2010.
- Hu, Q. H., Xie, Z. Q., Wang, X. M., Kang, H., He, Q. F., and Zhang, P.: Secondary organic aerosols over oceans via oxidation of isoprene and monoterpenes from Arctic to Antarctic, *Sci. Rep.-UK*, 3, 3119, <https://doi.org/10.1038/srep02280>, 2013.
- Huang, R. J., Zhang, Y.-L., Bozzetti, C., Ho, K.-F., Cao, J.-J., Han, Y., Daellenbach, K. R., Slowik, J. G., Platt, S. M., Canonaco, F., Zotter, P., Wolf, R., Pieber, S. M., Bruns, E. A., Crippa, M., Ciarelli, G., Piazzalunga, A., Schwikowski, M., Abbaszade, G., Schnelle-Kreis, J., Zimmermann, R., An, Z., Szidat, S., Baltensperger, U., Haddad, I. E., and Prévôt, A. S. H.: High secondary aerosol contribution to particulate pollution during haze events in China, *Nature*, 514, 218–222, <https://doi.org/10.1038/nature13774>, 2014.
- Huebert, B. J., Bates, T., Russell, P. B., Shi, G. Y., Kim, Y. J., Kawamura, K., Carmichael, G., and Nakajima, T.: An overview of ACE-Asia: Strategies for quantifying the relationships between Asian aerosols and their climatic impacts, *J. Geophys. Res.-Atmos.*, 108, 8633, <https://doi.org/10.1029/2003JD003550>, 2003.
- Jia, Y. L. and Fraser, M.: Characterization of saccharides in size-fractionated ambient particulate matter and aerosol sources: The contribution of primary biological aerosol particles (PBAPs) and soil to ambient particulate matter, *Environ. Sci. Technol.*, 45, 930–936, <https://doi.org/10.1021/es103104e>, 2011.
- Kanakidou, M., Seinfeld, J. H., Pandis, S. N., Barnes, I., Dentener, F. J., Facchini, M. C., Van Dingenen, R., Ervens, B., Nenes, A., Nielsen, C. J., Swietlicki, E., Putaud, J. P., Balkanski, Y., Fuzzi, S., Horth, J., Moortgat, G. K., Winterhalter, R., Myhre, C. E. L., Tsigaridis, K., Vignati, E., Stephanou, E. G., and Wilson, J.: Organic aerosol and global climate modelling: a review, *Atmos. Chem. Phys.*, 5, 1053–1123, <https://doi.org/10.5194/acp-5-1053-2005>, 2005.
- Kang, M., Ren, L., Ren, H., Zhao, Y., Kawamura, K., Zhang, H., Wei, L., Sun, Y., Wang, Z., and Fu, P.: Primary biogenic and anthropogenic sources of organic aerosols in Beijing, China: Insights from saccharides and n-alkanes, *Environ. Pollut.*, 243, 1579–1587, <https://doi.org/10.1016/j.envpol.2018.09.118>, 2018a.
- Kang, M., Fu, P., Kawamura, K., Yang, F., Zhang, H., Zang, Z., Ren, H., Ren, L., Zhao, Y., Sun, Y., and Wang, Z.: Characterization of biogenic primary and secondary organic aerosols in the marine atmosphere over the East China Sea, *Atmos. Chem. Phys.*, 18, 13947–13967, <https://doi.org/10.5194/acp-18-13947-2018>, 2018b.
- Kawamura, K., Kobayashi, M., Tsubonuma, N., Mochida, M., Watanabe, T., and Lee, M.: Organic and inorganic compositions of marine aerosols from East Asia: Seasonal variations of water-soluble dicarboxylic acids, major ions, total carbon and nitrogen, and stable C and N isotopic composition, in: *Geochemical investigations in earth and space science: A Tribute to Isaac R. Kaplan*, edited by: Hill, R. J., Leventhal, J., Aizenshtat, Z., Baedeker, M. J., Claypool, G., Eganhouse, R., Goldhaber, M., and Peters, K., The Geochemical Society, Publications Series No. 9, Elsevier, 243–265, 2004.
- Kessler, S. H., Smith, J. D., Che, D. L., Worsnop, D. R., Wilson, K. R., and Kroll, J. H.: Chemical sinks of organic aerosol: Kinetics and products of the heterogeneous oxidation of erythritol and levoglucosan, *Environ. Sci. Technol.*, 44, 7005–7010, <https://doi.org/10.1021/Es101465m>, 2010.
- Kleindienst, T. E., Jaoui, M., Lewandowski, M., Offenberg, J. H., Lewis, C. W., Bhawe, P. V., and Edney, E. O.: Estimates of the contributions of biogenic and anthropogenic hydrocarbons to secondary organic aerosol at a southeastern US location, *Atmos. Environ.*, 41, 8288–8300, 2007.
- Kourtchev, I., Hellebust, S., Bell, J. M., O'Connor, I. P., Healy, R. M., Allan, A., Healy, D., Wenger, J. C., and Sodeau, J. R.: The use of polar organic compounds to estimate the contribution of domestic solid fuel combustion and biogenic sources to ambient levels of organic carbon and PM_{2.5} in Cork Harbour, Ireland, *Sci. Total Environ.*, 11, 2143–2155, <https://doi.org/10.1016/j.scitotenv.2011.02.027>, 2011.
- Kroll, J. H., Ng, N. L., Murphy, S. M., Flagan, R. C., and Seinfeld, J. H.: Secondary organic aerosol formation from isoprene photooxidation under high-NO_x conditions, *Geophys. Res. Lett.*, 32, L18808, <https://doi.org/10.1029/2005gl023637>, 2005.
- Kroll, J. H., Ng, N. L., Murphy, S. M., Flagan, R. C., and Seinfeld, J. H.: Secondary organic aerosol formation from isoprene photooxidation, *Environ. Sci. Technol.*, 40, 1869–1877, 2006.
- Kundu, S., Kawamura, K., and Lee, M.: Seasonal variations of diacids, ketoacids, and α -dicarbonyls in aerosols at Gosan, Jeju Island, South Korea: Implications for sources, formation, and degradation during long-range transport, *J. Geophys. Res.*, 115, D19307, <https://doi.org/10.1029/2010jd013973>, 2010.
- Liu, J., Chu, B., Chen, T., Liu, C., Wang, L., Bao, X., and He, H.: Secondary organic aerosol formation from ambient air at an urban site in Beijing: Effects of OH exposure and precursor concentrations, *Environ. Sci. Technol.*, 52, 6834–6841, <https://doi.org/10.1021/acs.est.7b05701>, 2018.
- Medeiros, P. M. and Simoneit, B. R. T.: Analysis of sugars in environmental samples by gas chromatography-mass spectrometry, *J. Chromatogr. A*, 1141, 271–278, <https://doi.org/10.1016/j.chroma.2006.12.017>, 2007.
- Medeiros, P. M., Conte, M. H., Weber, J. C., and Simoneit, B. R. T.: Sugars as source indicators of biogenic organic carbon in aerosols collected above the Howland Experimental Forest, Maine, *Atmos. Environ.*, 40, 1694–1705, 2006.
- Mohn, J., Szidat, S., Fellner, J., Rechberger, H., Quartier, R., Buchmann, B., and Emmenegger, L.: Determination of biogenic and fossil CO₂ emitted by waste incineration based on ¹⁴CO₂ and mass balances, *Bioresour. Technol.*, 99, 6471–6479, <https://doi.org/10.1016/j.biortech.2007.11.042>, 2008.
- Müller, L., Reinnig, M.-C., Naumann, K. H., Saathoff, H., Mentel, T. F., Donahue, N. M., and Hoffmann, T.: Formation of

- 3-methyl-1,2,3-butanetricarboxylic acid via gas phase oxidation of pinonic acid – a mass spectrometric study of SOA aging, *Atmos. Chem. Phys.*, 12, 1483–1496, <https://doi.org/10.5194/acp-12-1483-2012>, 2012.
- Nakajima, T., Yoon, S. C., Ramanathan, V., Shi, G. Y., Take-mura, T., Higurashi, A., Takamura, T., Aoki, K., Sohn, B. J., Kim, S. W., Tsuruta, H., Sugimoto, N., Shimizu, A., Tani-moto, H., Sawa, Y., Lin, N. H., Lee, C. T., Goto, D., and Schut-gens, N.: Overview of the atmospheric brown cloud east Asian regional experiment 2005 and a study of the aerosol direct radiative forcing in east Asia, *J. Geophys. Res.-Atmos.*, 112, D24S91, <https://doi.org/10.1029/2007JD009009>, 2007.
- Ng, N. L., Kwan, A. J., Surratt, J. D., Chan, A. W. H., Chhabra, P. S., Sorooshian, A., Pye, H. O. T., Crounse, J. D., Wennberg, P. O., Flagan, R. C., and Seinfeld, J. H.: Secondary organic aerosol (SOA) formation from reaction of isoprene with ni-trate radicals (NO_3), *Atmos. Chem. Phys.*, 8, 4117–4140, <https://doi.org/10.5194/acp-8-4117-2008>, 2008.
- Offenberg, J., Lewis, C., Lewandowski, M., Jaoui, M., Kleindi-enst, T. E., and Edney, E. O.: Contributions of toluene and α -pinene to SOA formed in an irradiated toluene/ α -pinene/ NO_x /air mixture: Comparison of results using ^{14}C content and SOA or-ganic tracer methods, *Environ. Sci. Technol.*, 41, 3972–3976, 2007.
- Pashynska, V., Vermeylen, R., Vas, G., Maenhaut, W., and Claeys, M.: Development of a gas chromatographic/ion trap mass spectrometric method for the determination of levoglucosan and saccharidic compounds in atmospheric aerosols. Application to urban aerosols, *J. Mass Spectrom.*, 37, 1249–1257, 2002.
- Pio, C., Legrand, M., Alves, C. A., Oliveira, T., Afonso, J., Ca-seiro, A., Puxbaum, H., Sánchez-Ochoa, A., and Gelencsér, A.: Chemical composition of atmospheric aerosols during the 2003 summer intense forest fire period, *Atmos. Environ.*, 42, 7530–7543, 2008.
- Ramanathan, V., Li, F., Ramana, M. V., Praveen, P. S., Kim, D., Corrigan, C. E., Nguyen, H., Stone, E. A., Schauer, J. J., Carmichael, G. R., Adhikary, B., and Yoon, S. C.: At-mospheric brown clouds: Hemispherical and regional variations in long-range transport, absorption, and ra-diative forcing, *J. Geophys. Res.-Atmos.*, 112, D22S21, <https://doi.org/10.1029/2006JD008124>, 2007.
- Robinson, A. L., Donahue, N. M., Shrivastava, M. K., Weitkamp, E. A., Sage, A. M., Grieshop, A. P., Lane, T. E., Pierce, J. R., and Pandis, S. N.: Rethinking organic aerosols: Semivolatile emissions and photochemical aging, *Science*, 315, 1259–1262, 2007.
- Salazar, G., Zhang, Y. L., Agrios, K., and Szidat, S.: Development of a method for fast and automatic radiocarbon measurement of aerosol samples by online coupling of an elemental analyzer with a MICADAS AMS, *Nucl. Instrum. Meth. B*, 361, 163–167, <https://doi.org/10.1016/j.nimb.2015.03.051>, 2015.
- Schmidl, C., Bauer, H., Dattler, A., Hitznerberger, R., Weissenboeck, G., Marr, I. L., and Puxbaum, H.: Chemical characterisation of particle emissions from burning leaves, *Atmos. Environ.*, 42, 9070–9079, <https://doi.org/10.1016/J.Atmosenv.2008.09.010>, 2008a.
- Schmidl, C., Marr, I. L., Caseiro, A., Kotianova, P., Berner, A., Bauer, H., Kasper-Giebl, A., and Puxbaum, H.: Chemical charac-terisation of fine particle emissions from wood stove combustion of common woods growing in mid-European Alpine regions, *At-mos. Environ.*, 42, 126–141, 2008b.
- Shaw, S. L., Gantt, B., and Meskhidze, N.: Production and emis-sions of marine isoprene and monoterpenes: A Review, *Adv. Meteorol.*, 2010, 408696, <https://doi.org/10.1155/2010/408696>, 2010.
- Sheesley, R. J., Schauer, J. J., Chowdhury, Z., Cass, G. R., and Simoneit, B. R. T.: Characterization of organic aerosols emitted from the combustion of biomass in-digenous to South Asia, *J. Geophys. Res.*, 108, 4285, <https://doi.org/10.1029/2002JD002981>, 2003.
- Simoneit, B. R. T.: Biomass burning-a review of organic tracers for smoke from incomplete combustion, *Appl. Geochem.*, 17, 129–162, 2002.
- Simoneit, B. R. T., Schauer, J. J., Nolte, C. G., Oros, D. R., Elias, V. O., Fraser, M. P., Rogge, W. F., and Cass, G. R.: Levoglucosan, a tracer for cellulose in biomass burning and atmospheric particles, *Atmos. Environ.*, 33, 173–182, [https://doi.org/10.1016/S1352-2310\(98\)00145-9](https://doi.org/10.1016/S1352-2310(98)00145-9), 1999.
- Simoneit, B. R. T., Elias, V. O., Kobayashi, M., Kawamura, K., Rushdi, A. I., Medeiros, P. M., Rogge, W. F., and Didyk, B. M.: Sugars-dominant water-soluble organic compounds in soils and characterization as tracers in atmospheric particulate matter, *En-viron. Sci. Technol.*, 38, 5939–5949, 2004a.
- Simoneit, B. R. T., Kobayashi, M., Mochida, M., Kawamura, K., Lee, M., Lim, H.-J., Turpin, B. J., and Komazaki, Y.: Composi-tion and major sources of organic compounds of aerosol par-ticulate matter sampled during the ACE-Asia campaign, *J. Geo-phys. Res.*, 109, D19S10, <https://doi.org/10.1029/2004jd004598>, 2004b.
- Singh, N., Mhawish, A., Deboudt, K., Singh, R. S., and Baner-jee, T.: Organic aerosols over Indo-Gangetic Plain: Sources, dis-tributions and climatic implications, *Atmos. Environ.*, 157, 59–74, <https://doi.org/10.1016/j.atmosenv.2017.03.008>, 2017.
- Stein, A. F., Draxler, R. R., Rolph, G. D., Stunder, B. J. B., Co-hen, M. D., and Ngan, F.: NOAA's hysplit atmospheric trans-port and dispersion modeling system, *B. Am. Meteorol. Soc.*, 96, 2059–2077, <https://doi.org/10.1175/BAMS-D-14-00110.1>, 2015.
- Stuiver, M. and Polach, H. A.: Discussion: Reporting of ^{14}C data, *Radiocarbon*, 19, 355–363, 1997.
- Sullivan, A. P., Holden, A. S., Patterson, L. A., McMeeking, G. R., Kreidenweis, S. M., Malm, W. C., Hao, W. M., Wold, C. E., and Collett Jr., J. L.: A method for smoke marker measure-ments and its potential application for determining the contri-bution of biomass burning from wildfires and prescribed fires to ambient $\text{PM}_{2.5}$ organic carbon, *J. Geophys. Res.*, 113, D22302, <https://doi.org/10.1029/2008JD010216>, 2008.
- Surratt, J. D., Murphy, S. M., Kroll, J. H., Ng, N. L., Hildebrandt, L., Sorooshian, A., Szmigielski, R., Vermeylen, R., Maenhaut, W., Claeys, M., Flagan, R. C., and Seinfeld, J. H.: Chemical compo-sition of secondary organic aerosol formed from the photooxida-tion of isoprene, *J. Phys. Chem. A*, 110, 9665–9690, 2006.
- Surratt, J. D., Chan, A. W. H., Eddingsaas, N. C., Chan, M. N., Loza, C. L., Kwan, A. J., Hersey, S. P., Flagan, R. C., Wennberg, P. O., and Seinfeld, J. H.: Reactive intermediates re-vealed in secondary organic aerosol formation from isoprene, *P. Natl. Acad. Sci. USA*, 107, 6640–6645, 2010.

- Szidat, S., Jenk, T. M., Synal, H. A., Kalberer, M., Wacker, L., Hajas, I., Kasper-Giebl, A., and Baltensperger, U.: Contributions of fossil fuel, biomass-burning, and biogenic emissions to carbonaceous aerosols in Zurich as traced by ^{14}C , *J. Geophys. Res.-Atmos.*, 111, D07206, <https://doi.org/10.1029/2005JD006590>, 2006.
- Szmigielski, R., Surratt, J. D., Gómez-González, G., Van der Veken, P., Kourtchev, I., Vermeylen, R., Blockhuys, F., Jaoui, M., Kleindienst, T. E., Lewandowski, M., Offenberg, J. H., Edney, E. O., Seinfeld, J. H., Maenhaut, W., and Claeys, M.: 3-Methyl-1,2,3-butanetricarboxylic acid: An atmospheric tracer for terpene secondary organic aerosol, *Geophys. Res. Lett.*, 34, L24811, <https://doi.org/10.1029/2007GL031338>, 2007.
- Theodosi, C., Panagiotopoulos, C., Nouara, A., Zampas, P., Nicolaou, P., Violaki, K., Kanakidou, M., Sempéré, R., and Mihalopoulos, N.: Sugars in atmospheric aerosols over the Eastern Mediterranean, *Prog. Oceanogr.*, 163, 70–81, <https://doi.org/10.1016/j.pocean.2017.09.001>, 2018.
- Tyagi, P., Kawamura, K., Kariya, T., Bikkina, S., Fu, P., and Lee, M.: Tracing atmospheric transport of soil microorganisms and higher plant waxes in the East Asian outflow to the North Pacific Rim by using hydroxy fatty acids: Year-round observations at Gosan, Jeju Island, *J. Geophys. Res.*, 122, 4112–4131, <https://doi.org/10.1002/2016JD025496>, 2017.
- Verma, S. K., Kawamura, K., Chen, J., Fu, P., and Zhu, C.: Thirteen years of observations on biomass burning organic tracers over Chichijima Island in the western North Pacific: An outflow region of Asian aerosols, *J. Geophys. Res.*, 120, 4155–4168, <https://doi.org/10.1002/2014JD022224>, 2015.
- Verma, S. K., Kawamura, K., Chen, J., and Fu, P.: Thirteen years of observations on primary sugars and sugar alcohols over remote Chichijima Island in the western North Pacific, *Atmos. Chem. Phys.*, 18, 81–101, <https://doi.org/10.5194/acp-18-81-2018>, 2018.
- Wang, G. and Kawamura, K.: Molecular characteristics of urban organic aerosols from Nanjing: A case study of a mega-city in China, *Environ. Sci. Technol.*, 39, 7430–7438, 2005.
- Wang, G. H., Kawamura, K., and Lee, M.: Comparison of organic compositions in dust storm and normal aerosol samples collected at Gosan, Jeju Island, during spring 2005, *Atmos. Environ.*, 43, 219–227, <https://doi.org/10.1016/J.Atmosenv.2008.09.046>, 2009.
- Wang, G. H., Li, J. J., Cheng, C. L., Zhou, B. H., Xie, M. J., Hu, S. Y., Meng, J. J., Sun, T., Ren, Y. Q., Cao, J. J., Liu, S. X., Zhang, T., and Zhao, Z. Z.: Observation of atmospheric aerosols at Mt. Hua and Mt. Tai in central and east China during spring 2009 – Part 2: Impact of dust storm on organic aerosol composition and size distribution, *Atmos. Chem. Phys.*, 12, 4065–4080, <https://doi.org/10.5194/acp-12-4065-2012>, 2012.
- Wang, W., Kourtchev, I., Graham, B., Cafmeyer, J., Maenhaut, W., and Claeys, M.: Characterization of oxygenated derivatives of isoprene related to 2-methyltetrols in Amazonian aerosols using trimethylsilylation and gas chromatography/ion trap mass spectrometry, *Rapid Commun. Mass Sp.*, 19, 1343–1351, 2005.
- Wang, Y. Q., Zhang, X. Y., and Draxler, R. R.: TrajStat: GIS-based software that uses various trajectory statistical analysis methods to identify potential sources from long-term air pollution measurement data, *Environ. Modell. Softw.*, 24, 938–939, <https://doi.org/10.1016/j.envsoft.2009.01.004>, 2009.
- Wu, J., Kong, S., Zeng, X., Cheng, Y., Yan, Q., Zheng, H., Yan, Y., Zheng, S., Liu, D., Zhang, X., Fu, P., Wang, S., and Qi, S.: First high-resolution emission inventory of levoglucosan for biomass burning and non-biomass burning sources in China, *Environ. Sci. Technol.*, 55, 3, 1497–1507, 2021.
- Yan, C., Zheng, M., Sullivan, A. P., Shen, G., Chen, Y., Wang, S., Zhao, B., Cai, S., Desyaterik, Y., Li, X., Zhou, T., Gustafsson, Ö., and Collett, J. L.: Residential coal combustion as a source of levoglucosan in China, *Environ. Sci. Technol.*, 52, 3, 1665–1674, <https://doi.org/10.1021/acs.est.7b05858>, 2018.
- Yttri, K. E., Dye, C., and Kiss, G.: Ambient aerosol concentrations of sugars and sugar-alcohols at four different sites in Norway, *Atmos. Chem. Phys.*, 7, 4267–4279, <https://doi.org/10.5194/acp-7-4267-2007>, 2007.
- Zangrando, R., Barbaro, E., Kirchgeorg, T., Vecchiato, M., Scalabrin, E., Radaelli, M., Đorđević, D., Barbante, C., and Gambaro, A.: Five primary sources of organic aerosols in the urban atmosphere of Belgrade (Serbia), *Sci. Total Environ.*, 571, 1441–1453, <https://doi.org/10.1016/j.scitotenv.2016.06.188>, 2016.
- Zhang, Y. L., Perron, N., Ciobanu, V. G., Zotter, P., Mingüilón, M. C., Wacker, L., Prévôt, A. S. H., Baltensperger, U., and Szidat, S.: On the isolation of OC and EC and the optimal strategy of radiocarbon-based source apportionment of carbonaceous aerosols, *Atmos. Chem. Phys.*, 12, 10841–10856, <https://doi.org/10.5194/acp-12-10841-2012>, 2012.
- Zhang, Y.-L., Huang, R.-J., El Haddad, I., Ho, K.-F., Cao, J.-J., Han, Y., Zotter, P., Bozzetti, C., Daellenbach, K. R., Canonaco, F., Slowik, J. G., Salazar, G., Schwikowski, M., Schnelle-Kreis, J., Abbaszade, G., Zimmermann, R., Baltensperger, U., Prévôt, A. S. H., and Szidat, S.: Fossil vs. non-fossil sources of fine carbonaceous aerosols in four Chinese cities during the extreme winter haze episode of 2013, *Atmos. Chem. Phys.*, 15, 1299–1312, <https://doi.org/10.5194/acp-15-1299-2015>, 2015.
- Zhang, Y. L., Kawamura, K., Agrios, K., Lee, M., Salazar, G., and Szidat, S.: Fossil and nonfossil sources of organic and elemental carbon aerosols in the outflow from Northeast China, *Environ. Sci. Technol.*, 50, 6284–6292, <https://doi.org/10.1021/acs.est.6b00351>, 2016.
- Zhu, C., Kawamura, K., and Kunwar, B.: Effect of biomass burning over the western North Pacific Rim: wintertime maxima of anhydrosugars in ambient aerosols from Okinawa, *Atmos. Chem. Phys.*, 15, 1959–1973, <https://doi.org/10.5194/acp-15-1959-2015>, 2015a.
- Zhu, C., Kawamura, K., and Kunwar, B.: Organic tracers of primary biological aerosol particles at subtropical Okinawa island in the western North Pacific rim, *J. Geophys. Res.*, 120, 5504–5523, <https://doi.org/10.1002/2015JD023611>, 2015b.